

690  
LYLE LUTTON

TECHNICAL NOTES

NATIONAL ADVISORY COMMITTEE FOR AERONAUTICS

690  
-----  
No. 690  
-----

# CASE FILE COPY

RÉSUMÉ OF AIR-LOAD DATA ON SLATS AND FLAPS

By Carl J. Wenzinger and Francis M. Rogallo  
Langley Memorial Aeronautical Laboratory

PROPERTY FAIRCROFT  
ENGINEERING LIBRARY

Washington  
March 1939

1977

1977

1977

1977

1977

1977

NATIONAL ADVISORY COMMITTEE FOR AERONAUTICS

TECHNICAL NOTE NO. 690

RÉSUMÉ OF AIR-LOAD DATA ON SLATS AND FLAPS

By Carl J. Wenzinger and Francis M. Rogallo

SUMMARY

A résumé of the generally available test data regarding air loads on slats and flaps is presented and data obtained up to the fall of 1938 are included. The data are given in the form of N.A.C.A. standard coefficients of air forces and moments on the lift-increasing device and, when available, the aerodynamic characteristics of the combined wing and high-lift device are included. Slats of the Handley Page type, fixed auxiliary airfoils, and flaps of several different types are covered.

INTRODUCTION

A study was made by the N.A.C.A. at the request of the Matériel Division, Army Air Corps, during the early part of 1934 to furnish information applicable to design criterions for slots and flaps of various types. The present report is a résumé of the generally available test data regarding air loads on slats and flaps and includes data obtained up to the fall of 1938.

The material includes data on slats of the Handley Page type of slotted wing; fixed auxiliary airfoils; and plain flaps, simple split flaps, split flaps at different chord locations, Zap flaps, N.A.C.A. slotted flaps, Fowler flaps, and external-airfoil flaps.

PRESENTATION OF DATA

The data are given in the form of N.A.C.A. standard coefficients of air forces and moments on the lift-increasing device and, when available, the aerodynamic characteristics of the combined wing and high-lift device are included. The data of the combination, in practically all

of the cases, have been corrected for the effects of the jet boundaries.

The coefficients used in this report were taken directly from the various references and are listed as follows:

- $C_L$ , total lift coefficient of the combination.
- $C_{N_w}$ , total normal-force coefficient of the combination.
- $C_D$ , total drag coefficient of the combination.
- $(c.p.)_w$ , center of pressure of wing, in percent chord.
- $(c.p.)_f$ , center of pressure of flap, in percent chord.
- $C_{N_{aux}}$ , total normal-force coefficient of auxiliary airfoil.
- $C_{C_{aux}}$ , total chord-force coefficient of auxiliary airfoil.
- $C_{N_f}$ , total normal-force coefficient of flap.
- $C_{h_f}$ , total hinge-moment coefficient of flap.
- $c_l$ , section lift coefficient of combination.
- $c_{n_w}$ , section normal-force coefficient of combination.
- $c_{d_o}$ , section profile-drag coefficient of combination.
- $c_{m(a.c.)_o}$ , section pitching-moment coefficient of combination about aerodynamic center of plain wing.
- $c_{n_s}$ , section normal-force coefficient of slat.
- $c_{n_f}$ , section normal-force coefficient of flap.
- $c_{c_f}$ , section chord-force coefficient of flap.
- $c_{h_f}$ , section hinge-moment coefficient of flap.

and

- $c_w$ , chord of wing.  
 $c_f$ , chord of flap.  
 $q$ , dynamic pressure.  
 $p/q$ , point pressure coefficient on surface of wing, slat, or flap.  
 $\alpha$ , angle of attack of wing, finite aspect ratio.  
 $\alpha_0$ , angle of attack of wing, infinite aspect ratio.

## LEADING-EDGE DEVICES

### Slots

Measurements have been made in the N.A.C.A. variable-density wind tunnel to determine the pressure distribution over the midspan section of an R.A.F. 31 wing with leading-edge slot full open (reference 1). Figures 1, 2, and 3 show representative pressure-distribution diagrams for the slotted wing with the slat completely extended. The pressures in these figures for both the slat and the main wing are plotted normal to the chord of the main wing.

Normal forces on the slat.— The normal-force coefficients obtained for the slat of the slotted R.A.F. 31 wing in terms of slat area are shown in figure 4. This figure also shows the variation of the wing normal force and center of pressure with the angle of attack of the wing. The measured value of the slat normal-force coefficient at the stalling angle of attack of the wing was about 2.4.

Resultant force on slat.— Several investigations have been made to determine the direction and the magnitude of the resultant force on the slat, mainly for the purpose of designing the automatic operating mechanism and the supporting linkage. Figure 5 is a vectorial representation of the slat forces. The vectors are drawn in their correct location and direction with respect to the slat chord for different angles of attack of the main wing. The magnitudes of the forces may be obtained directly from the lengths of the vectors. It should be noted that these values apply only to the particular wing and slat combination tested; separate tests will be required to obtain satis-

factory data for other wing and slat combinations. The aerodynamic characteristics of the slotted R.A.F. 31 airfoil are not available. A slotted Clark Y wing has been tested in the N.A.C.A. wind tunnels and the effects of slat position (reference 2) and of Reynolds Number (reference 3) upon the characteristics have been determined.

#### Auxiliary Airfoils (Fixed)

Aerodynamic characteristics obtained in the N.A.C.A. 7- by 10-foot wind tunnel for a Clark Y wing with an N.A.C.A. 22 auxiliary airfoil are given in figure 6. These data were taken from reference 4 and are directly comparable with similar data on wings with slots and flaps obtained in the same tunnel. Tests were made in the N.A.C.A. 5-foot vertical wind tunnel to determine the division of air load between a Clark Y main wing and fixed auxiliary airfoils of the N.A.C.A. 22 and the N.A.C.A. 0012 sections (reference 5). The arrangements tested and the results of these tests are shown in figures 7 and 8.

The highly cambered N.A.C.A. 22 auxiliary airfoil had higher normal-force coefficients throughout the range of lift coefficients of the combination investigated than did the symmetrical N.A.C.A. 0012 auxiliary airfoil, although the characteristics of the two combinations were about the same. Based on the total lift of the combination, the N.A.C.A. 0012 auxiliary airfoil carried about 20 percent of the total load throughout the range of lift coefficients tested, whereas the N.A.C.A. 22 auxiliary airfoil carried about the same proportion of the total load at high lift coefficients as the N.A.C.A. 0012 auxiliary airfoil but carried a higher proportion at low lift coefficients. No other load data for these devices are available.

#### TRAILING-EDGE DEVICES

##### Plain Flaps

Measurements have been made in the N.A.C.A. 7- by 10-foot wind tunnel to determine the aerodynamic effects of plain flaps on an N.A.C.A. 23012 wing (reference 6). The resultant characteristics shown in figure 9 were determined for an arrangement in which the gap between the flap and the wing was sealed because it has been shown (refer-

ence 6) that even a relatively small gap has a detrimental effect on the lift and the drag.

Pressure-distribution measurements have also been made in the 7- by 10-foot wind tunnel of an N.A.C.A. 23012 wing with a 20-percent-chord plain flap (reference 7). A comparison is given in figure 10 of the pressure distribution over a plain wing with that over the flapped wing at three different flap settings. Figures 11 and 12 give the flap normal-force and hinge-moment coefficients and centers of pressure for various flap deflections from  $45^\circ$  up to  $75^\circ$  down. It will be noted that deflections of the flap to the limits tested produce a progressive increase in the normal force on the flap up to the stalling angle of the wing. The maximum value of the normal-force coefficient obtained at the  $75^\circ$  deflection is 1.6, although the maximum lift of the wing was not reached at this point. For flaps of other chord lengths and for serially hinged flaps, a method of computing the flap loads and the hinge moments is given in reference 8.

### Simple Split Flaps

#### Normal forces and centers of pressure on the flap.--

Direct measurements of the forces acting on split flaps and on the complete wing have been made in the N.A.C.A. 7- by 10-foot wind tunnel (reference 9). Clark Y wing models were used with two different sizes of full-span split flaps, one having a narrow chord (15 percent of the wing chord) and the other a medium chord (25 percent of the wing chord). The aerodynamic characteristics of the wing and flap combinations tested are given in figures 13 and 14.

Figures 15 and 16 show that the normal force on the split flaps increases both with flap deflection and with increase in lift of the combination. Below the stall, the maximum value of the normal-force coefficient (based on flap area) is about 1.4 and occurs at the angle of attack and the flap deflection for maximum lift of the combination with the  $0.15c_w$  flap ( $C_{L_{max}} = 2.06$ ). The center of pressure of the load on the split flaps, in general, moves forward with decrease in flap deflection and with increase in lift of the combination from small values of the lift up to the stall.

Hinge moments of the flap.— Moments about the flap hinge are plotted in figures 17 and 18 as coefficients of hinge moment based on flap chord and area. The magnitudes of these moments are practically the same for the two sizes of split flap tested and are about the same as those for similar sizes of plain flap. A method of computing the normal forces and the hinge moments of the flaps is given in reference 8 for split flaps having chords other than those mentioned.

#### Split Flaps at Various Chord Locations, Including the Zap Arrangement

A series of pressure-distribution tests was made in the N.A.C.A. full-scale wind tunnel over the mid-semispan section of an N.A.C.A. 2212 wing with split flaps on a Fairchild 22 airplane (reference 10). The data given herein are for a flap 20 percent of the wing chord located successively at 68, 80, and 89 percent of the wing chord from the leading edge. The farthest back location with the flap down for maximum lift corresponds to a Zap arrangement. Total normal-force coefficients and centers of pressure for the three arrangements noted are given in figures 19, 21, and 23. Normal-force coefficients for the flap and centers of pressure of the air load on the flap are given in figures 20, 22, and 24. These data show that the flap normal-force coefficients vary both with flap deflection and with normal force of the combination; they are relatively independent of hinge-axis location. The centers of pressure on the flap cover about the same range for the three arrangements considered and are practically unaffected by flap deflection, flap location, and normal force of the combination.

#### Slotted Flaps

Force tests have been made in the 7- by 10-foot wind tunnel (reference 11) on a 3-foot-chord N.A.C.A. 23012 wing with an N.A.C.A. slotted flap. Section characteristics from the force tests are given in figure 25 for flap deflections from  $0^\circ$  to  $60^\circ$  down. The loads on the flap were determined from a pressure-distribution investigation of a similar wing and flap combination (reference 7). Diagrams of the pressure distribution over the wing and the flap are given in figure 26 and the air loads acting on the flap are given in figure 27 in the form of normal- and chord-force coefficients and centers of pressure of the load act-

ing on the flap. The maximum value of the normal-force coefficient for this type of flap has a value of about 1.8, which is obtained with the  $40^\circ$  flap deflection. The chord-force coefficients are of appreciable magnitude and must be considered in the structural design of this flap.

### Fowler Flaps

An investigation (reference 12) was made in the N.A.C.A. 7- by 10-foot wind tunnel of a Clark Y wing with Fowler flaps having chords 20, 30, and 40 percent of the main wing chord. Aerodynamic characteristics of the wing with each of the three sizes of flap set for maximum lift are given in figure 28 together with the characteristics of a plain Clark Y wing. A pressure-distribution investigation was made of a Clark Y wing with a 20-percent-chord Clark Y Fowler flap and of an N.A.C.A. 23012 wing with 20-, 30-, and 40-percent chord N.A.C.A. 23012 Fowler flaps (reference 13). Comparisons of the pressure distribution over the wing and flap combinations for both the Clark Y and the N.A.C.A. 23012 Fowler flaps are given in figures 29 and 30. The normal- and the chord-force coefficients of the flap and the centers of pressure are shown in figure 31 for the various arrangements mentioned. The 20-percent-chord Clark Y Fowler flap and the 40-percent-chord N.A.C.A. 23012 Fowler flap gave the highest values of the normal-force coefficient. These coefficients have a value of about 1.35 and are the same for both sizes of flap. The chord-force coefficients of the Fowler flaps are considerably smaller than those of the N.A.C.A. slotted flap.

### External-Airfoil Flaps

Normal and chord forces and centers of pressure on the flap.- Force tests have been made in the N.A.C.A. 7- by 10-foot wind tunnel of an N.A.C.A. 23012 wing with a 20-percent-chord N.A.C.A. 23012 external-airfoil flap (reference 14). Aerodynamic characteristics of the wing and flap combination are given in figure 32 for several flap deflections.

A pressure-distribution investigation has also been made on the wing and flap combination (reference 15) in which the air loads on the main wing and the flap were measured. Pressure-distribution diagrams for the wing with external-airfoil flap are given in figures 33 and 34

for several different flap deflections and for both a constant normal force of the combination and a given angle of attack. Normal-force coefficients and centers of pressure on the flap are given in figure 35 for several deflections covering a range from the high-speed setting ( $-3^{\circ}$ ) to beyond that for maximum lift. The maximum normal-force coefficient for this type of flap has about the same value as that of the Fowler flap.

Hinge moments of the flap.— The moments about the flap hinge location shown are given in figure 36 as coefficients of hinge moment based on flap chord and area. This type of flap lends itself easily to aerodynamic balancing and the hinge axis used for the present arrangement gives probably the smallest practical hinge moments without overbalance.

Langley Memorial Aeronautical Laboratory,  
National Advisory Committee for Aeronautics,  
Langley Field, Va., January 12, 1939.

## REFERENCES

1. Jacobs, Eastman N.: Pressure Distribution on a Slotted R.A.F. 31 Airfoil in the Variable Density Wind Tunnel. T.N. No. 308, N.A.C.A., 1929.
2. Wenzinger, Carl J., and Shortal, Joseph A.: The Aerodynamic Characteristics of a Slotted Clark Y Wing as Affected by the Auxiliary Airfoil Position. T.R. No. 400, N.A.C.A., 1931.
3. Jacobs, Eastman N., and Sherman, Albert: Airfoil Section Characteristics as Affected by Variations of the Reynolds Number. T.R. No. 586, N.A.C.A., 1937.
4. Weick, Fred E., and Noyes, Richard W.: Wind-Tunnel Research Comparing Lateral Control Devices, Particularly at High Angles of Attack. X. Various Control Devices on a Wing with a Fixed Auxiliary Airfoil. T.N. No. 451, N.A.C.A., 1933.
5. Weick, Fred E., and Sanders, Robert: Wind-Tunnel Tests on Combinations of a Wing with Fixed Auxiliary Airfoils Having Various Chords and Profiles. T.R. No. 472, N.A.C.A., 1933.
6. Wenzinger, Carl J.: Wind-Tunnel Investigation of Ordinary and Split Flaps on Airfoils of Different Profile. T.R. No. 554, N.A.C.A., 1936.
7. Wenzinger, Carl J. and Delano, James B.: Pressure Distribution over an N.A.C.A. 23012 Airfoil with a Slotted and a Plain Flap. T.R. No. 633, N.A.C.A., 1938.
8. Allen, H. Julian: Calculation of the Chordwise Load Distribution over Airfoil Sections with Plain, Split, or Serially Hinged Trailing-Edge Flaps. T.R. No. 634, N.A.C.A., 1938.
9. Wenzinger, Carl J.: Wind-Tunnel Measurements of Air Loads on Split Flaps. T.N. No. 498, N.A.C.A., 1934.
10. Wallace, Rudolf: Investigation of Full-Scale Split Trailing-Edge Wing Flaps with Various Chords and Hinge Locations. T.R. No. 539, N.A.C.A., 1935.

11. Wenzinger, Carl J., and Bamber, Millard J.: Wind-Tunnel Tests of Three Lateral-Control Devices in Combination with a Full-Span Slotted Flap on an N.A.C.A. 23012 Airfoil. T.N. No. 659, N.A.C.A., 1938.
12. Platt, Robert C.: Aerodynamic Characteristics of a Wing with Fowler Flaps Including Flap Loads, Downwash, and Calculated Effect on Take-Off. T.R. No. 534, N.A.C.A., 1935.
13. Wenzinger, Carl J., and Anderson, Walter B.: Pressure Distribution over Airfoils with Fowler Flaps. T.R. No. 620, N.A.C.A., 1938.
14. Platt, Robert C., and Abbott, Ira H.: Aerodynamic Characteristics of N.A.C.A. 23012 and 23021 Airfoils with 20-Percent-Chord External-Airfoil Flaps of N.A.C.A. 23012 Section. T.R. No. 573, N.A.C.A., 1936.
15. Wenzinger, Carl J.: Pressure Distribution over an N.A.C.A. 23012 Airfoil with an N.A.C.A. 23012 External-Airfoil Flap. T.R. No. 614, N.A.C.A., 1938.

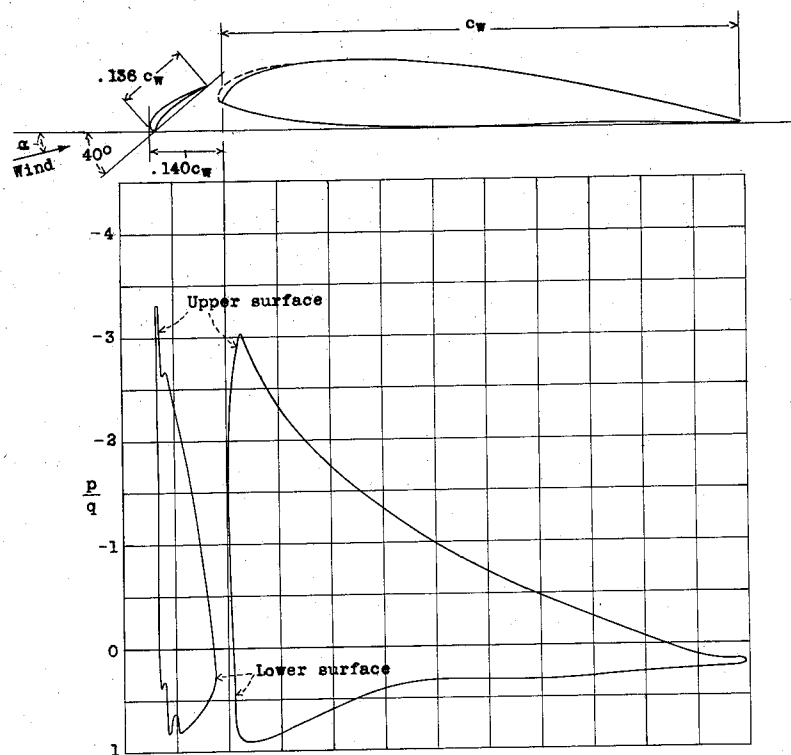


Figure 1.- Pressure-distribution diagram for slotted R.A.F. 31 wing,  $\alpha = 16^\circ$  (reference 1).

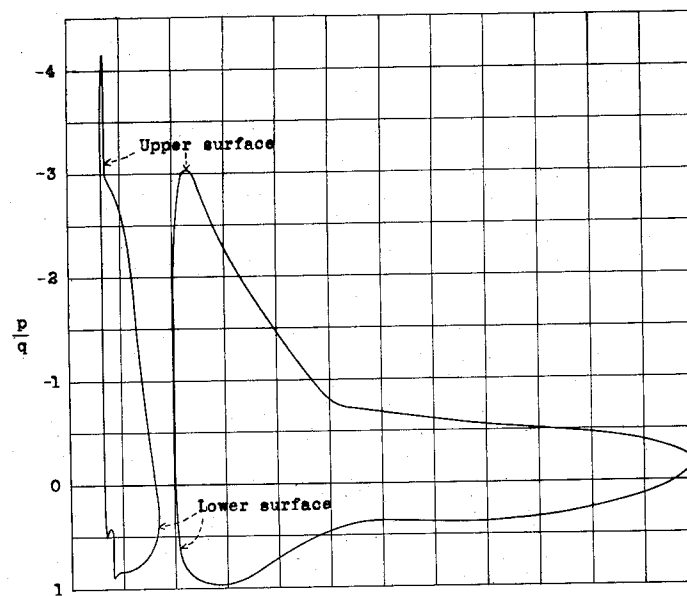


Figure 2. Pressure-distribution diagram for slotted R.A.F. 31 wing,  $\alpha = 25^\circ$  (reference 1).

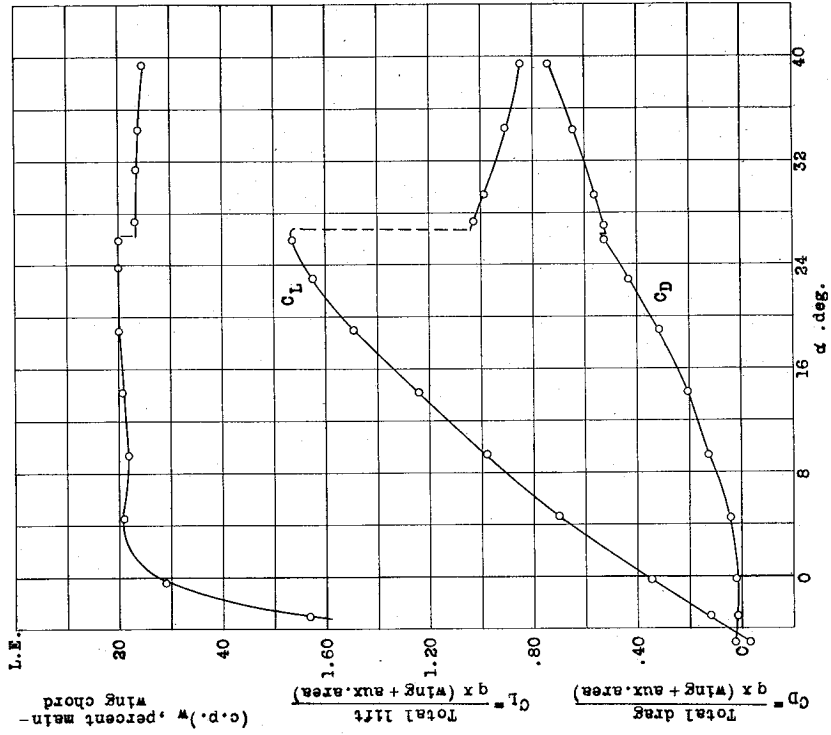
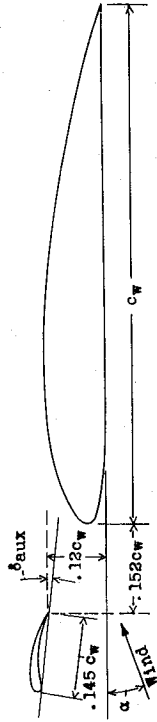


Figure 6.- Lift and drag coefficients and centers of pressure of a Clark Y wing with an N.A.C.A. 22 auxiliary airfoil;  $\delta_{aux}$ , 0° (reference 4).

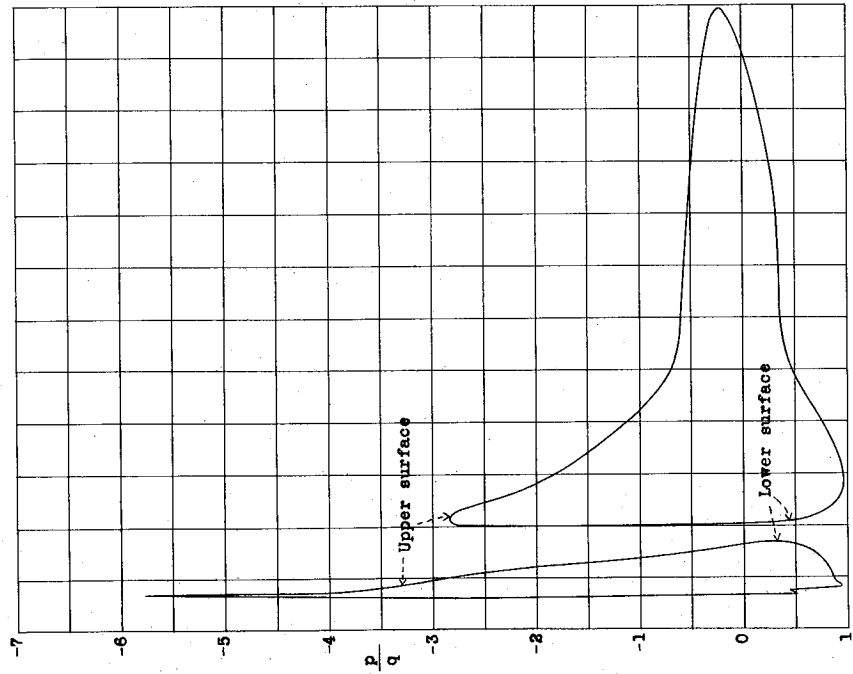


Figure 3.- Pressure-distribution diagram for slotted R.A.F. 31 wing,  $\alpha = 31^\circ$  (reference 1).

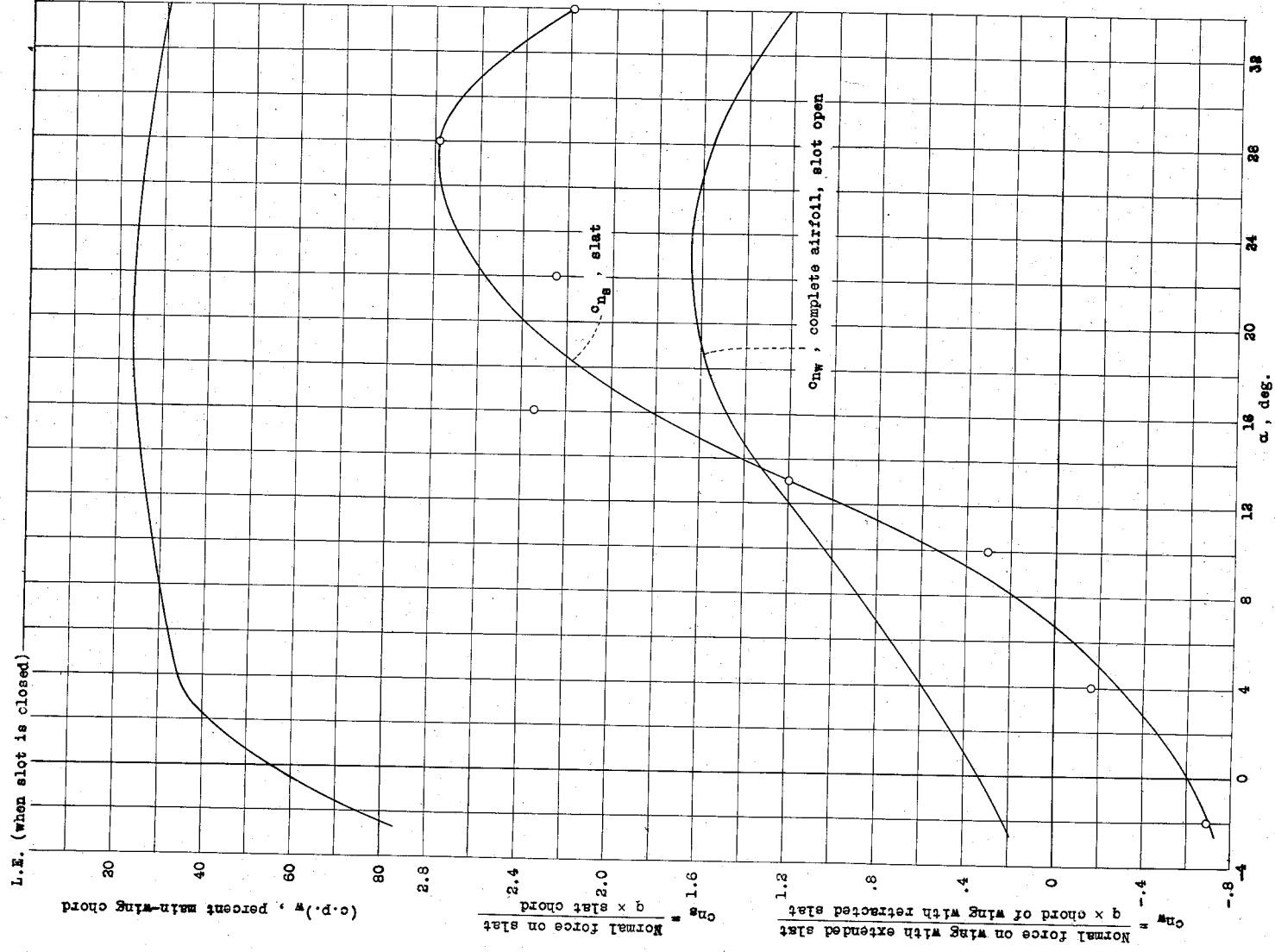


Figure 4.- Normal-force coefficients and centers of pressure of a slotted R.A.F. 31 wing, and normal-force coefficients of the slat, (reference 1).

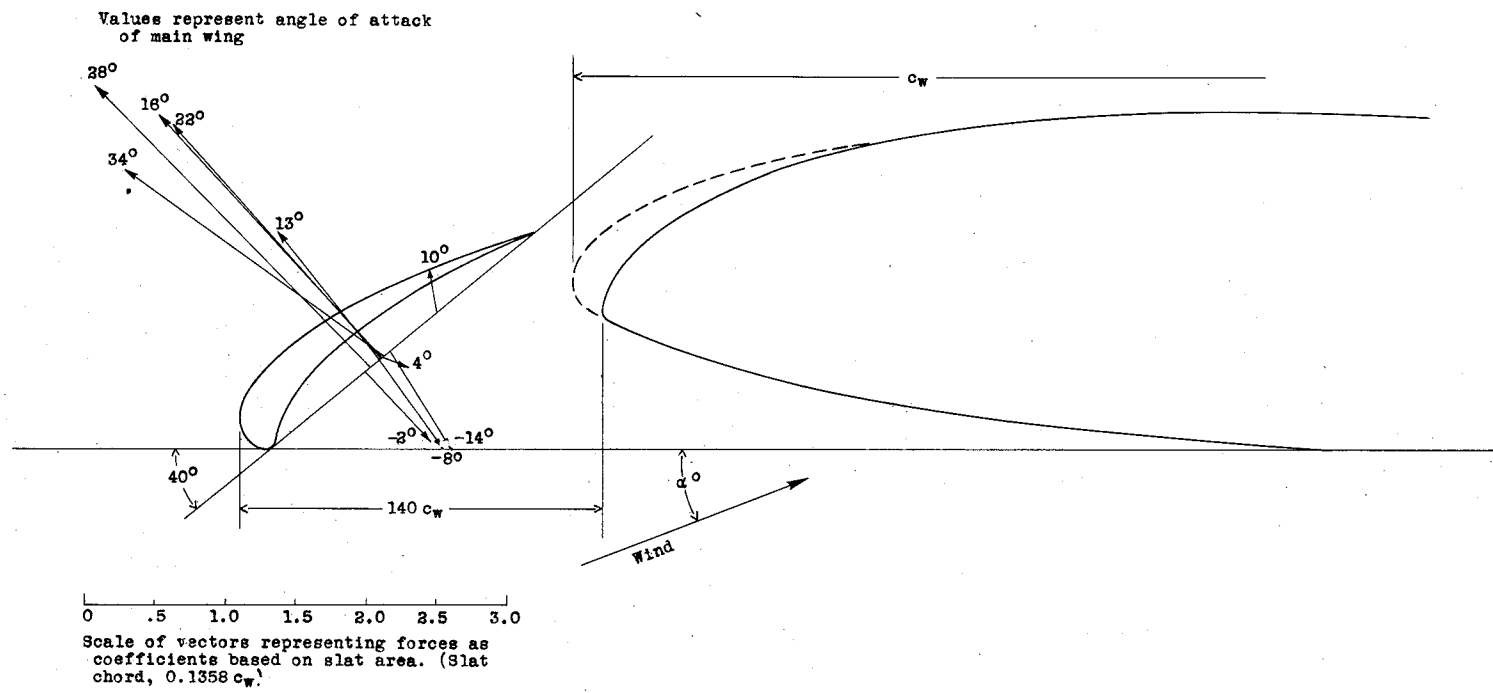


Figure 5. Vector diagram representing forces on slat with slot fully open (reference 1)

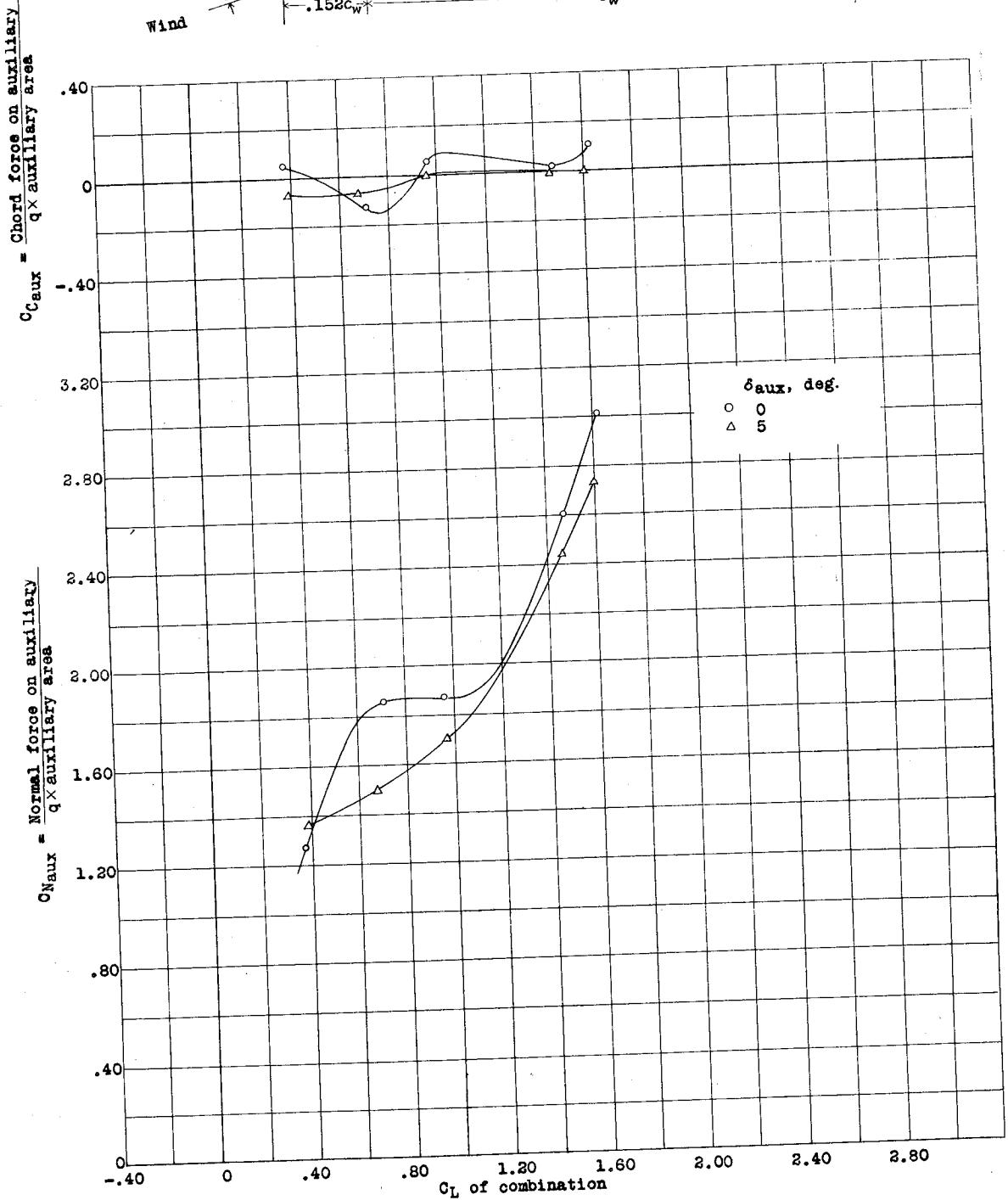
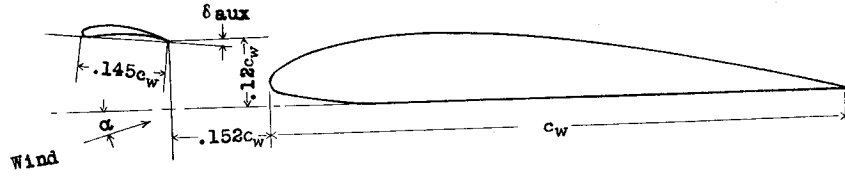


Figure 7.- Normal and chord-force coefficients of N.A.C.A. 22 auxiliary airfoil ahead of a Clark Y wing (reference 5).

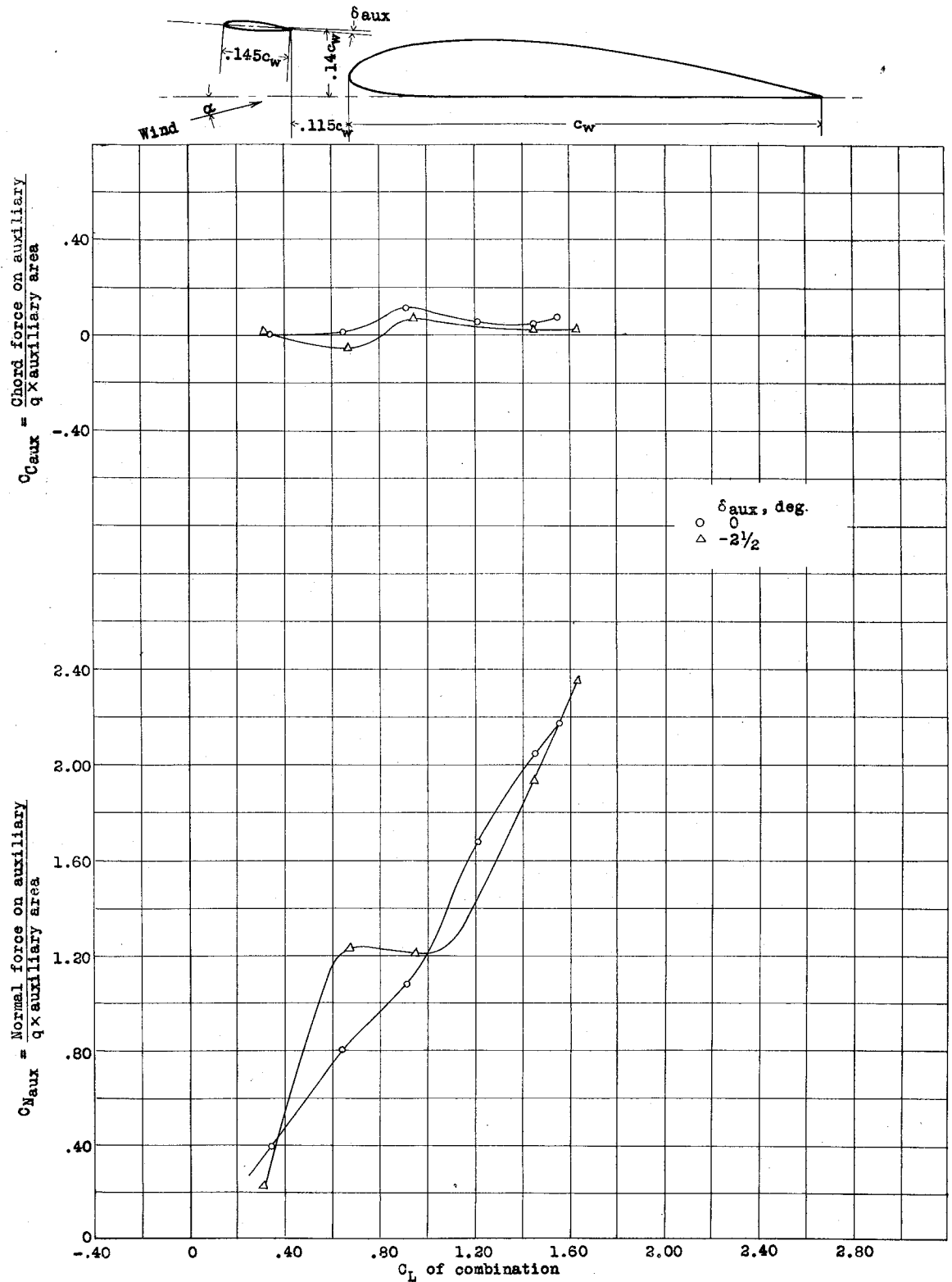


Figure 8.- Normal and chord-force coefficients of N.A.C.A. 0012 auxiliary airfoil ahead of a Clark Y wing (reference 5).

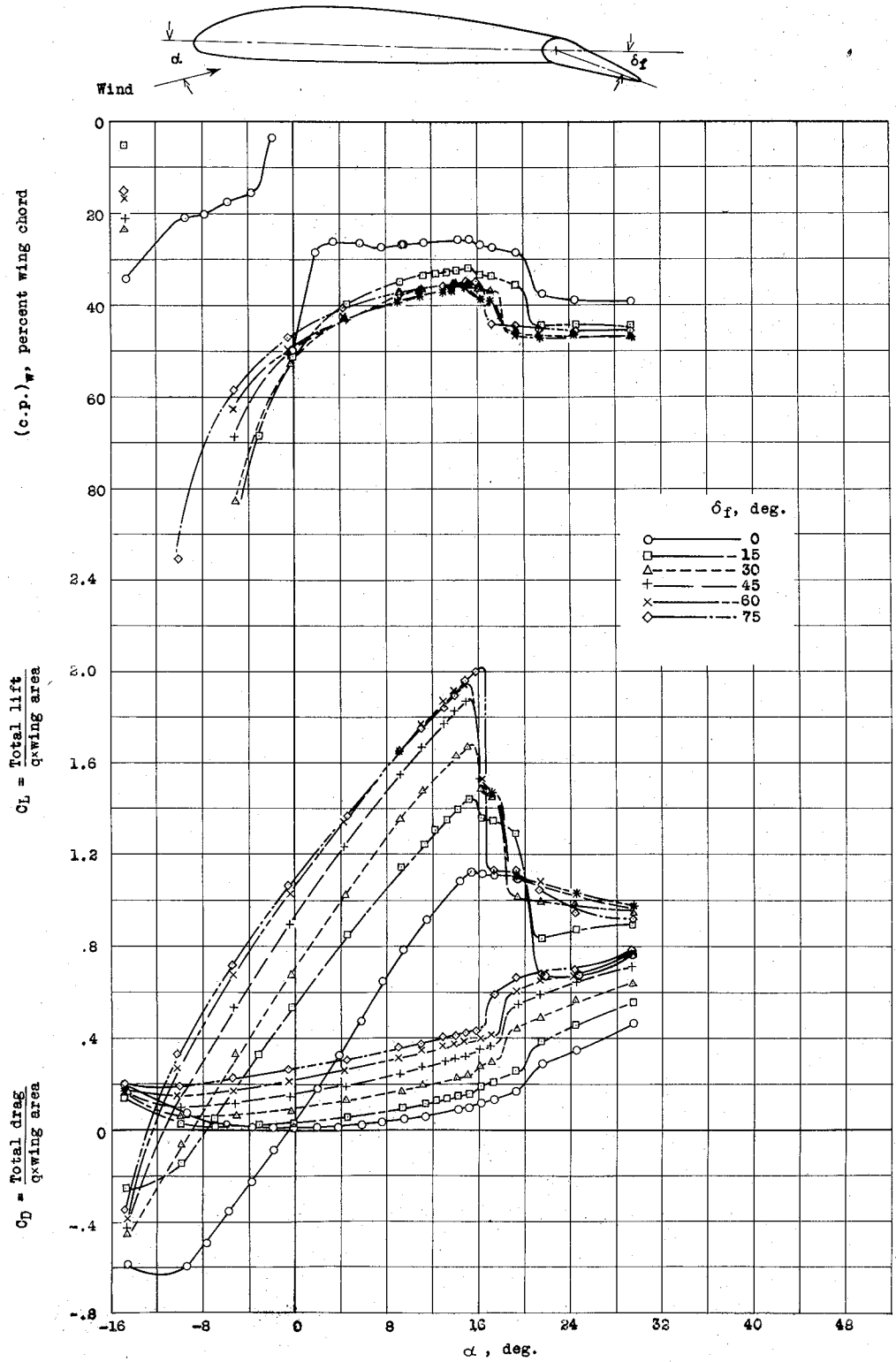


Figure 9.- Lift and drag coefficients and centers of pressure of an N.A.C.A. 23012 wing with a 0.20c<sub>w</sub> plain flap, (reference 6).

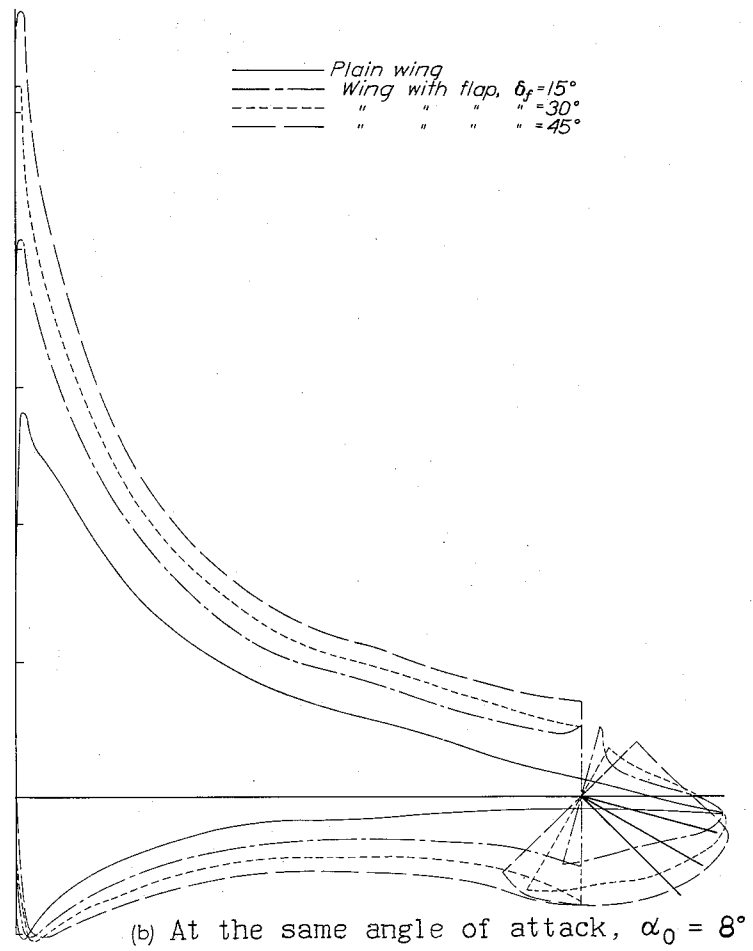
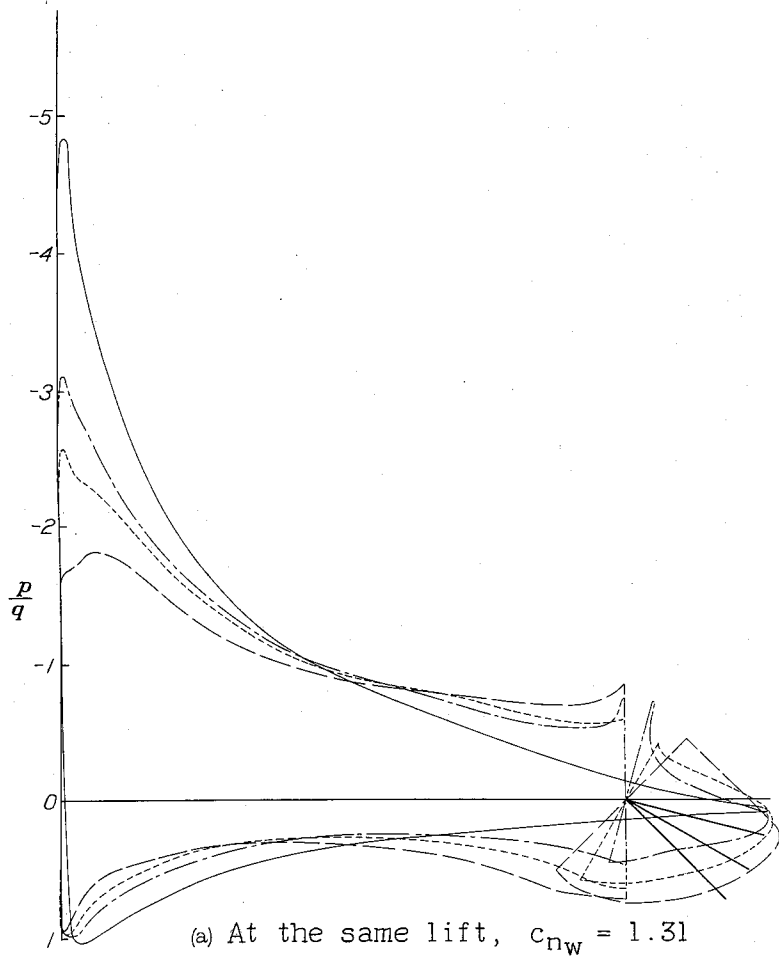


Figure 10.- Comparison of the pressure distribution on an N.A.C.A. 23012 wing and a 0.20  $c_w$  plain flap with that on the plain wing, (reference 7).

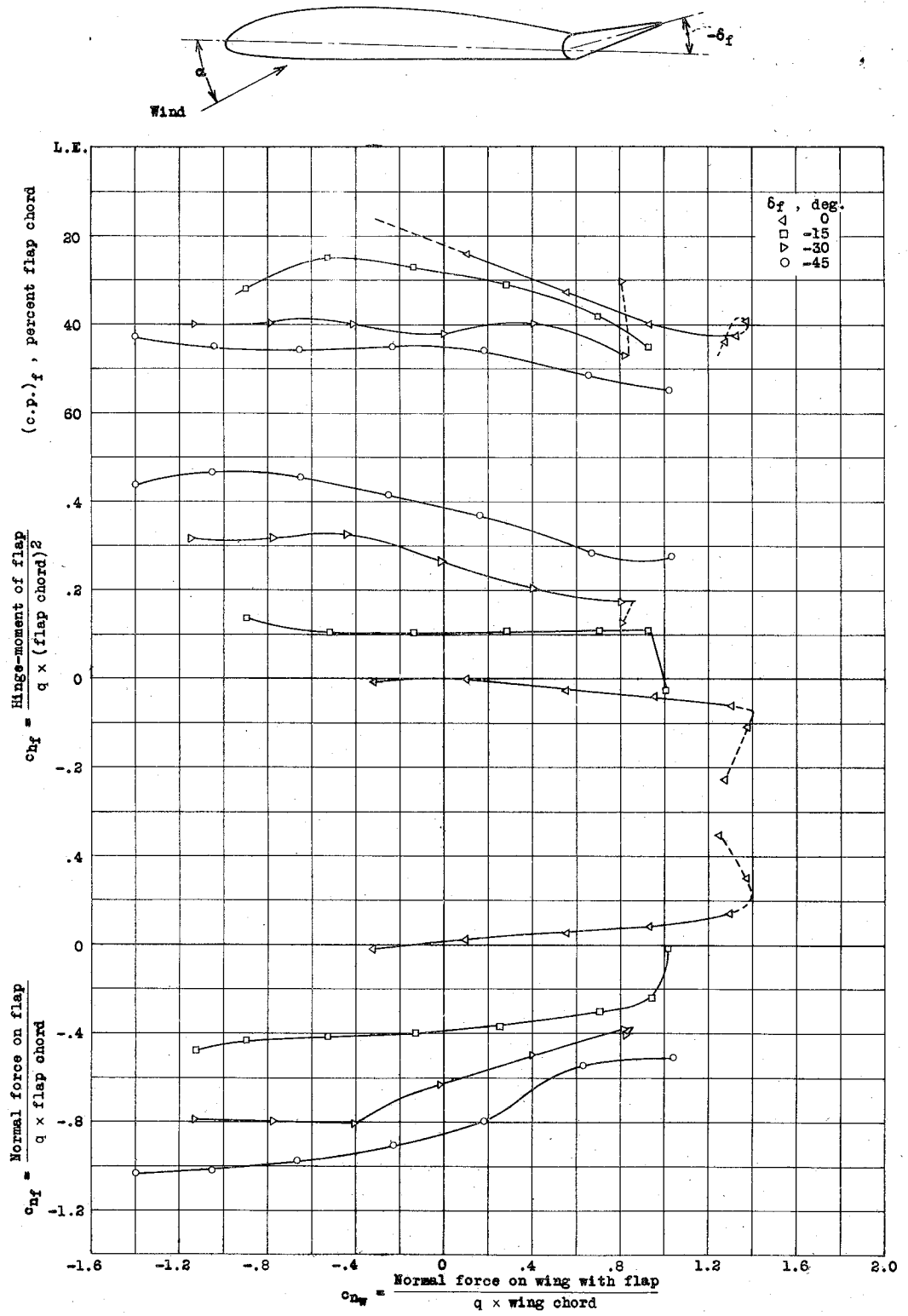


Figure 11.- Normal-force and hinge-moment coefficients, and centers of pressure of a 0.20  $c_w$  plain flap on an N.A.C.A. 23012 wing. Flap deflections from 0° to -45°, (reference 7).

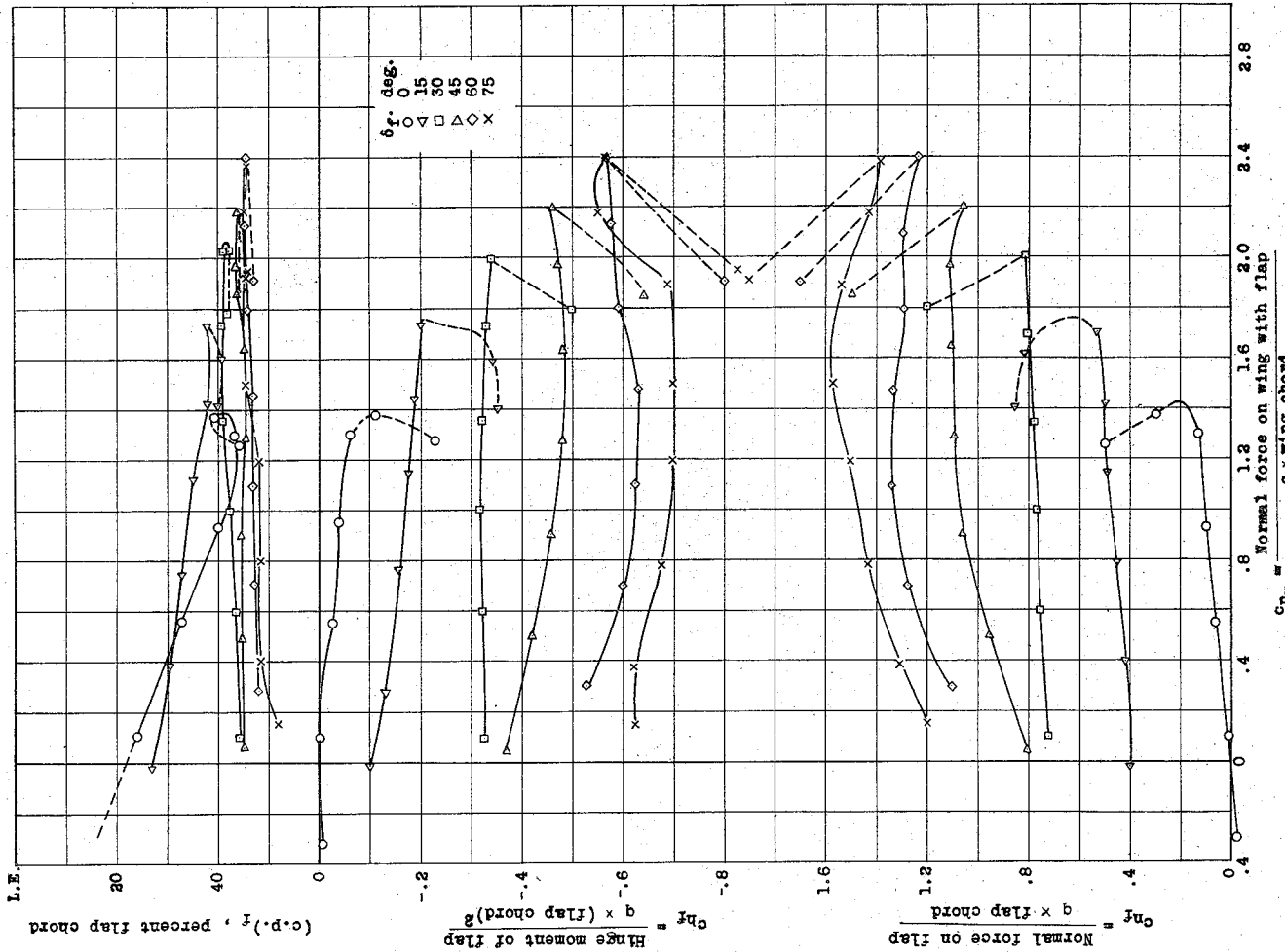


Figure 12. Normal-force and hinge-moment coefficients and centers of pressure of a 0.50 cw plain flap on an N.A.C.A. 23012 wing. Flap deflections from 0° to 75°. (reference 7)

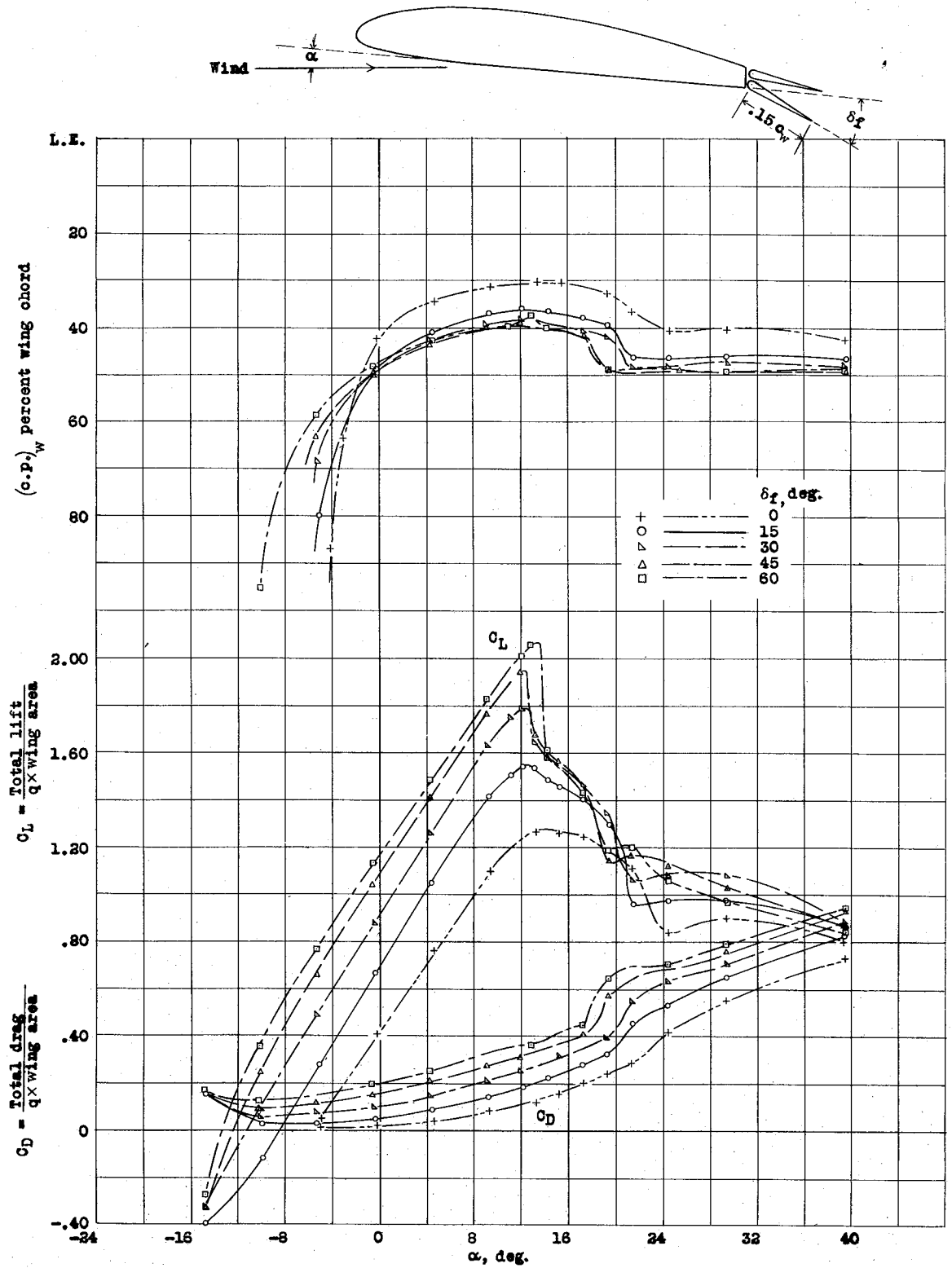


Figure 13.- Lift and drag coefficients and center of pressure of a Clark Y wing with a  $0.15c_w$  split flap (reference 9).

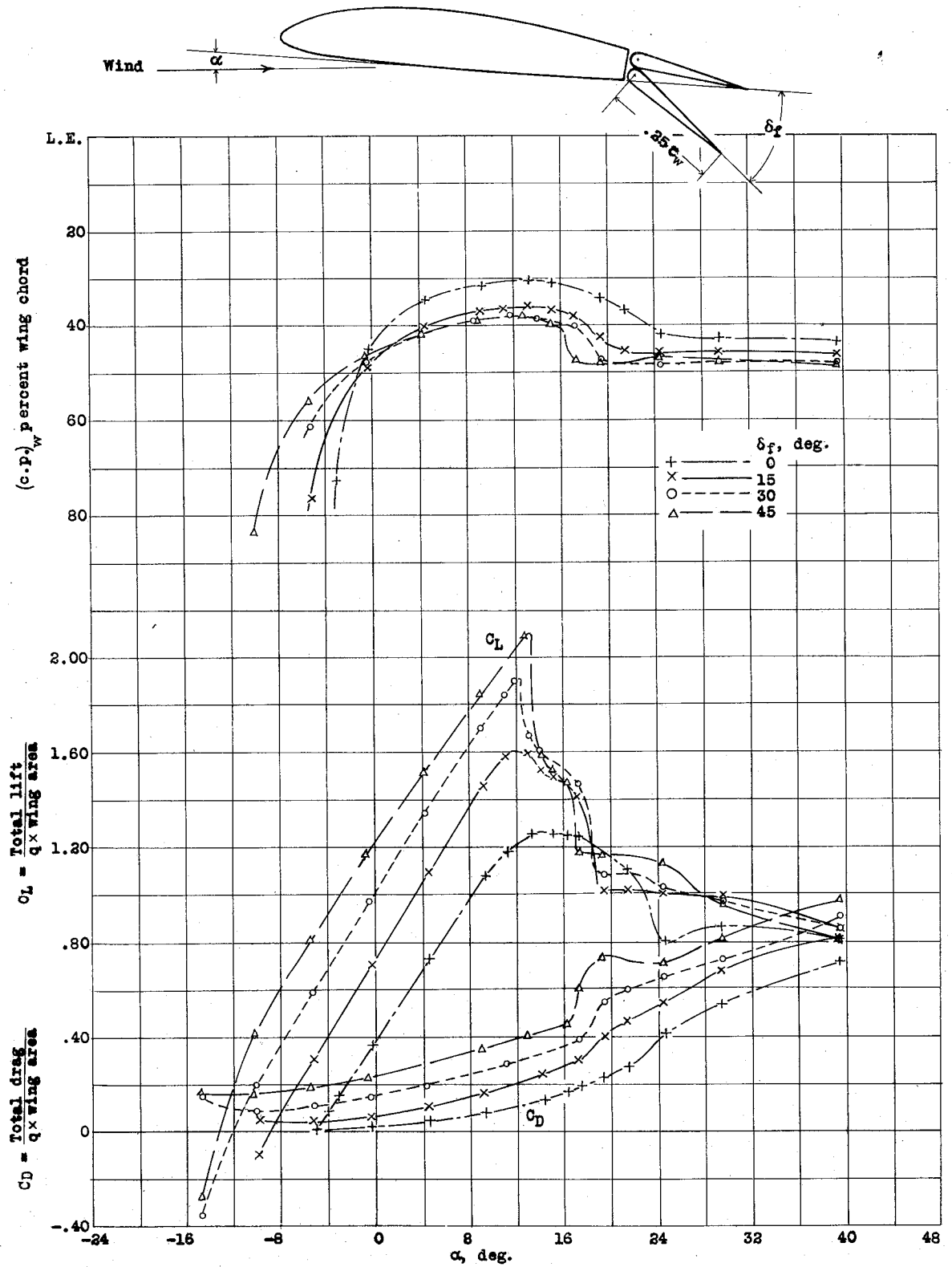


Figure 14.- Lift and drag coefficients and center of pressure of a Clark Y wing with a  $0.25c_w$  split flap (reference 9).

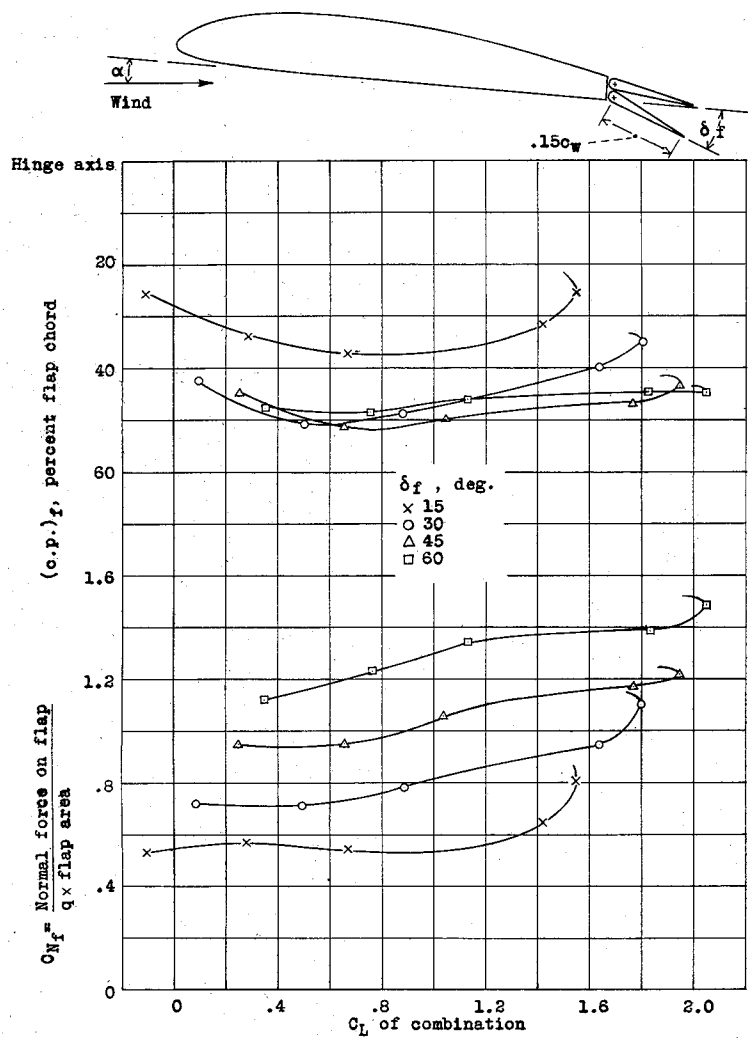


Figure 15.- Normal-force coefficients and centers of pressure of a  $0.15c_w$  split flap on a Clark Y wing, (reference 9).

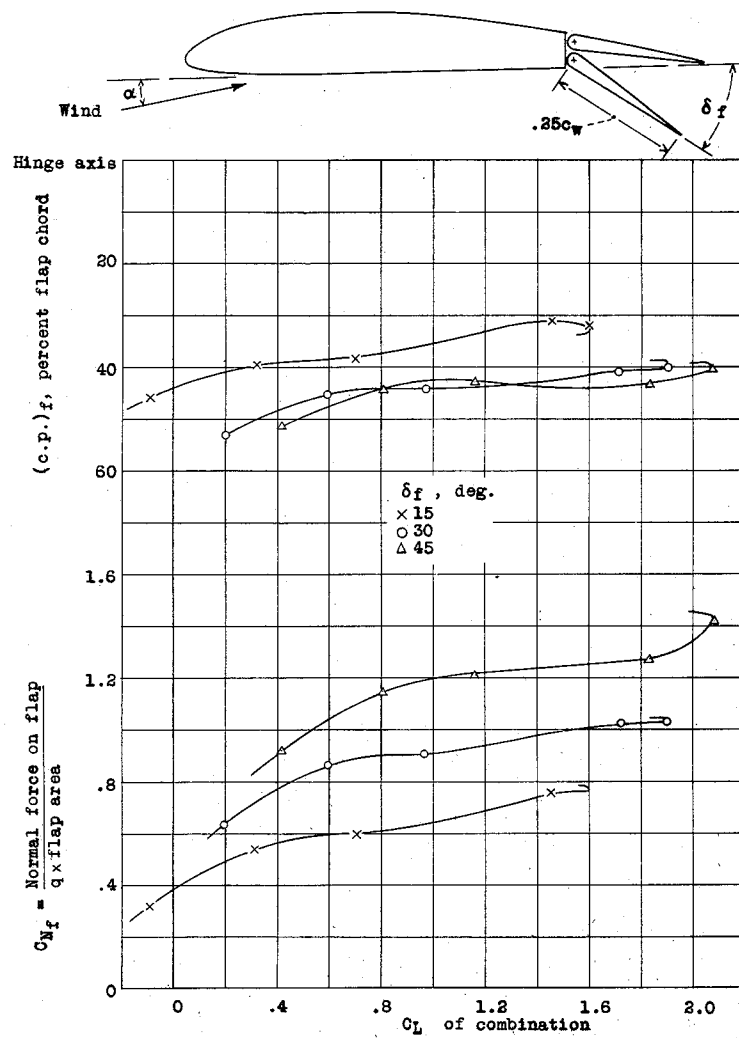


Figure 16.- Normal-force coefficients and centers of pressure of a  $0.25c_w$  split flap on a Clark Y wing, (reference 9).

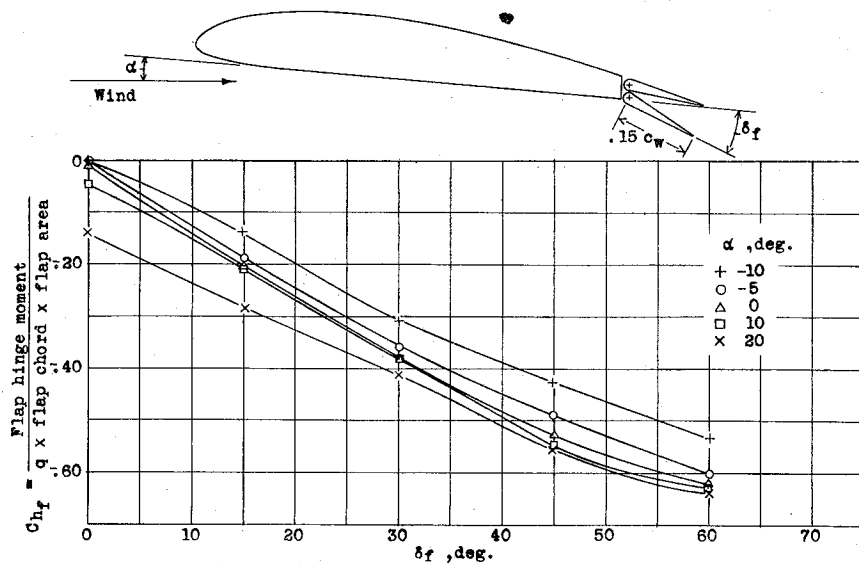


Figure 17. Hinge-moment coefficients of a  $0.15c_w$  split flap on a Clark Y wing (reference 9).

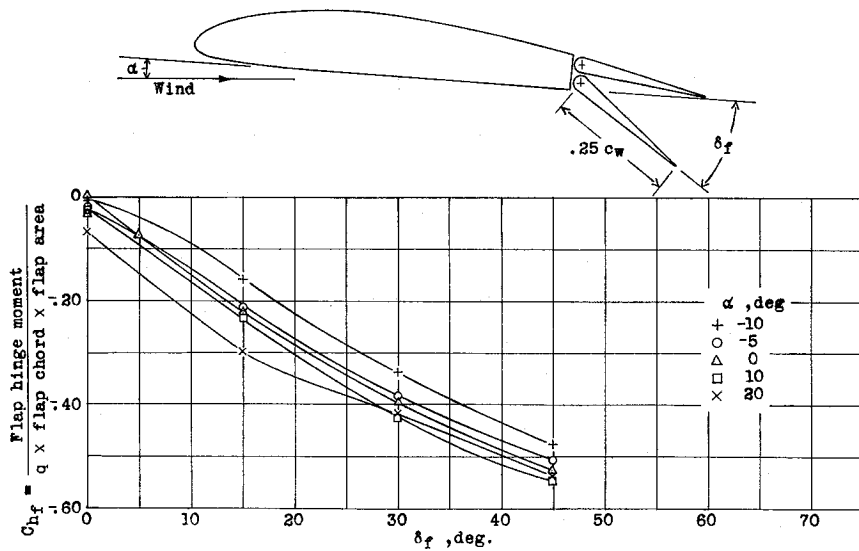


Figure 18. Hinge-moment coefficients of a  $0.25c_w$  split flap on a Clark Y wing (reference 9).

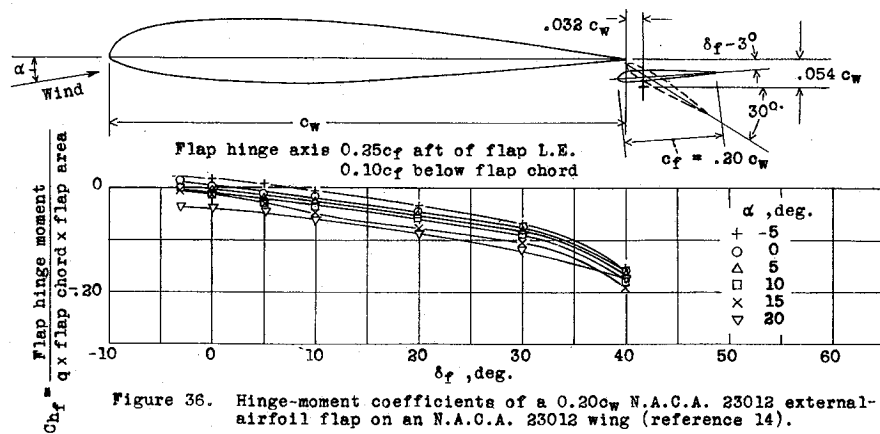


Figure 36. Hinge-moment coefficients of a  $0.20c_w$  N.A.C.A. 23012 external-airfoil flap on an N.A.C.A. 23012 wing (reference 14).

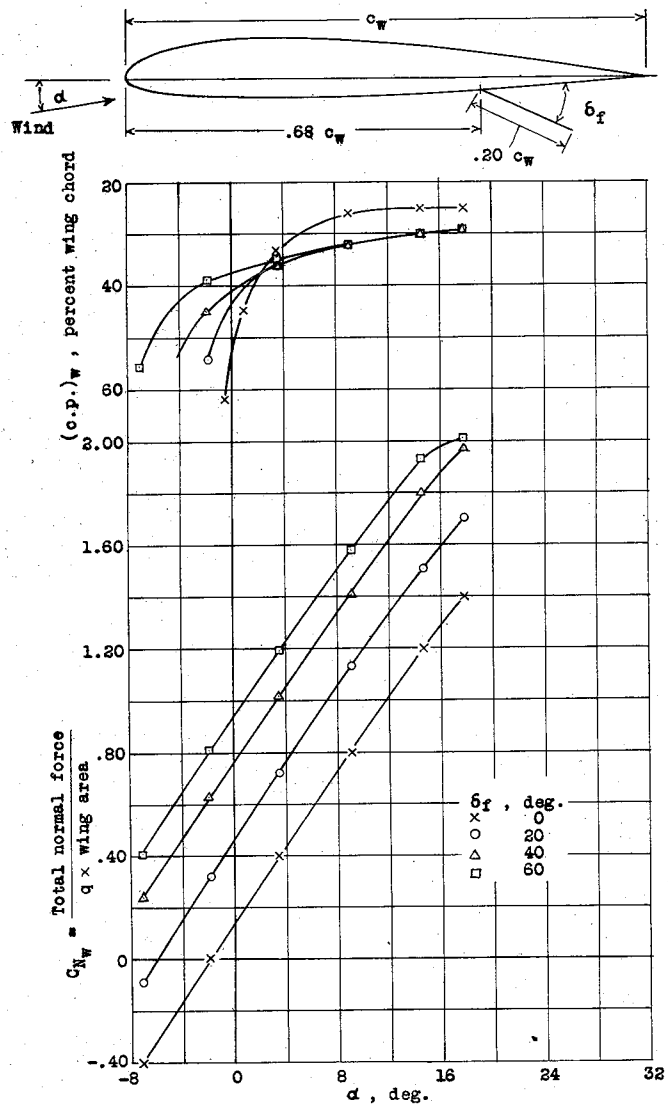


Figure 19.- Normal-force coefficients and centers of pressure of an N.A.C.A. 2312 wing with a  $0.20 c_w$  split flap at  $0.68 c_w$ , (reference 10).

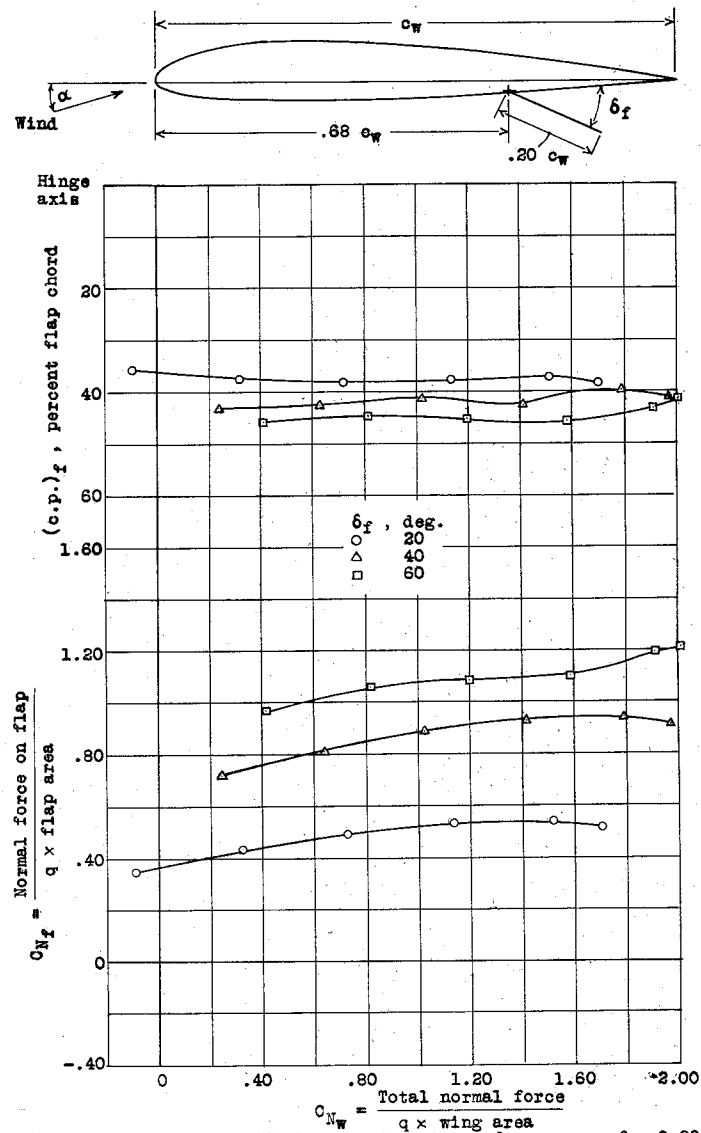


Figure 20.- Normal-force coefficients and centers of pressure of a  $0.20 c_w$  split flap at  $0.68 c_w$  on an N.A.C.A. 2312 wing, (reference 10).

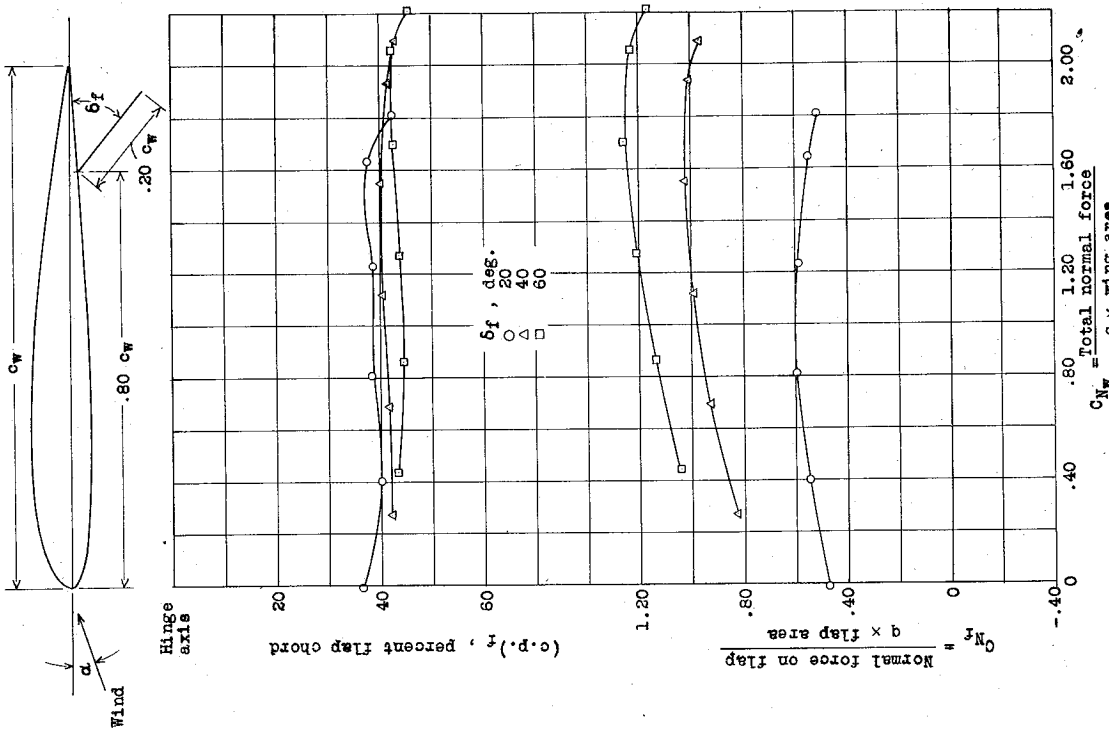


Figure 21.- Normal-force coefficients and centers of pressure of an N.A.C.A. 2212 wing with a 0.20  $c_w$  split flap at 0.80  $c_w$ , (reference 10).

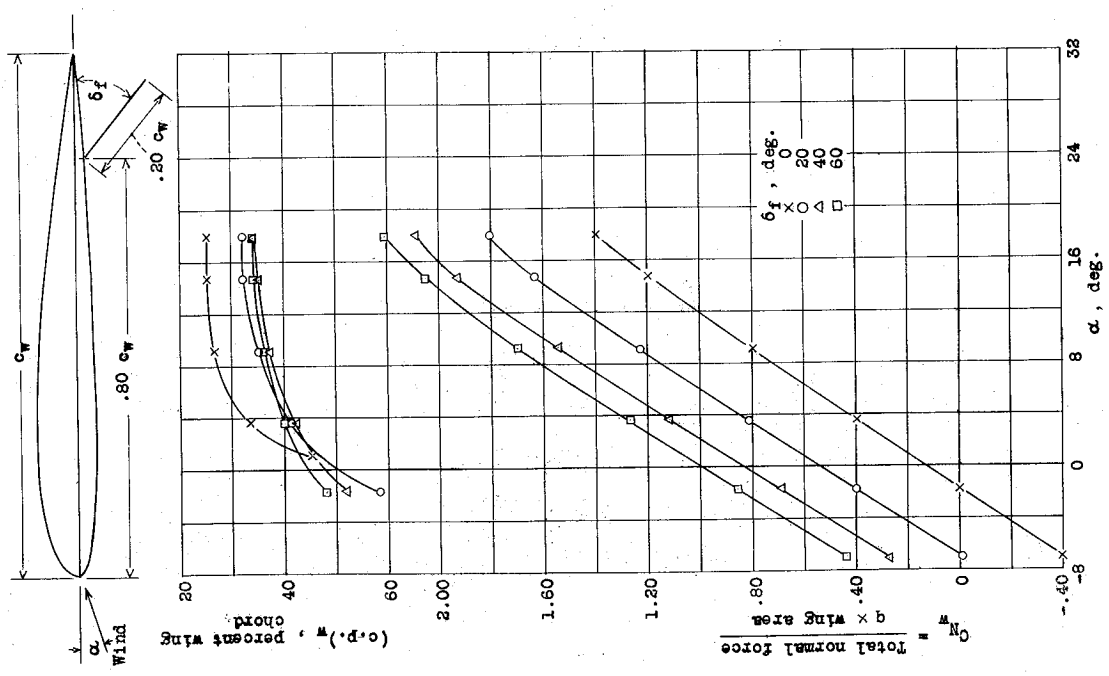


Figure 22.- Normal-force coefficients and centers of pressure of a 0.20- $c_w$  split flap at 0.80  $c_w$  on an N.A.C.A. 2212 wing, (reference 10).

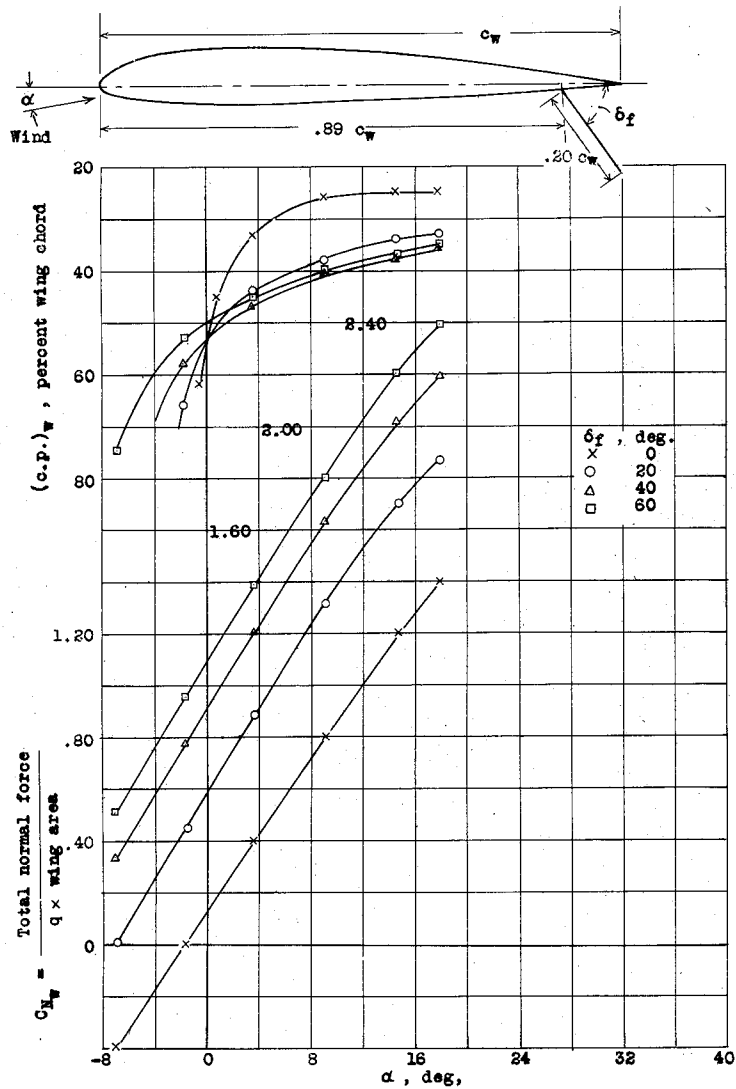


Figure 23.- Normal-force coefficients and centers of pressure of an N.A.C.A. 2212 wing with a  $0.20 c_w$  split flap (Zap) at  $0.89 c_w$ , (reference 10).

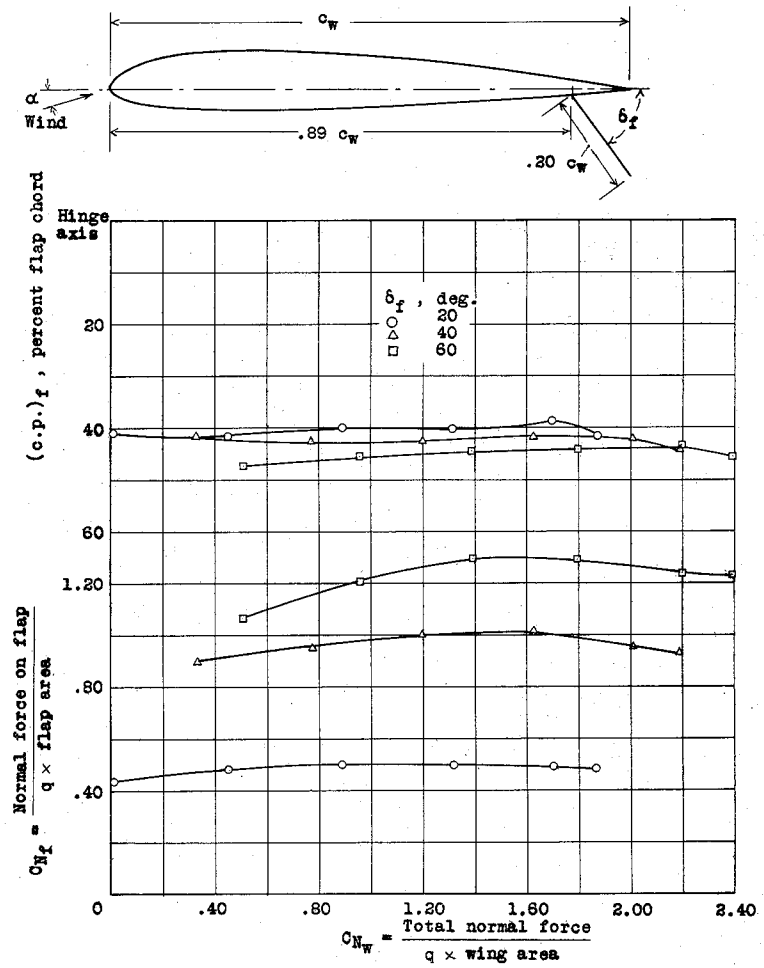


Figure 24.- Normal-force coefficients and centers of pressure of a  $0.20 c_w$  split flap (Zap) at  $0.89 c_w$  on an N.A.C.A. 2212 wing (reference 10).

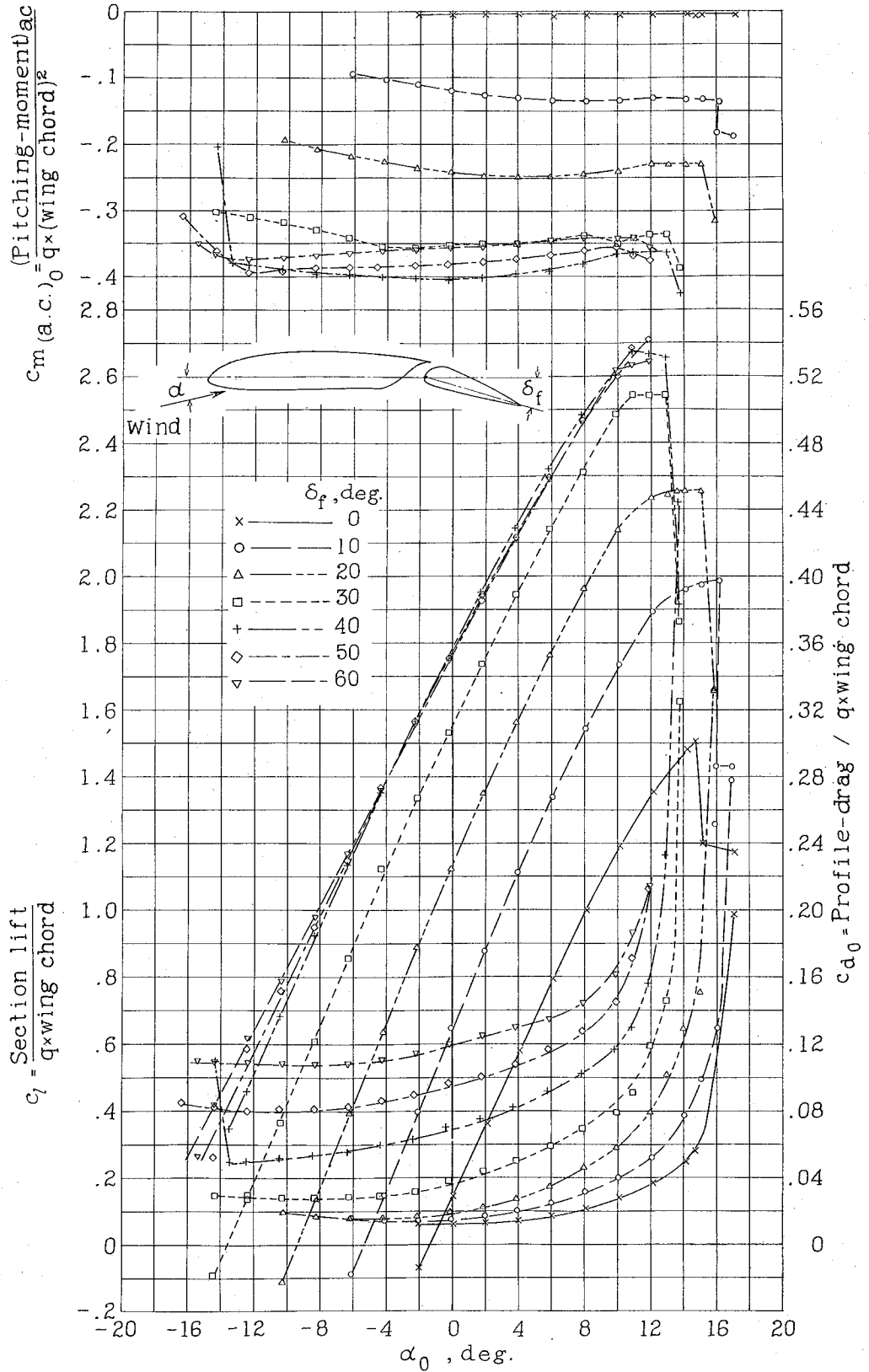


Figure 25.- Section lift, drag, and pitching-moment coefficients of an N.A.C.A. 23012 wing with a 0.2566<sub>c<sub>w</sub></sub> slotted flap. (reference 11)

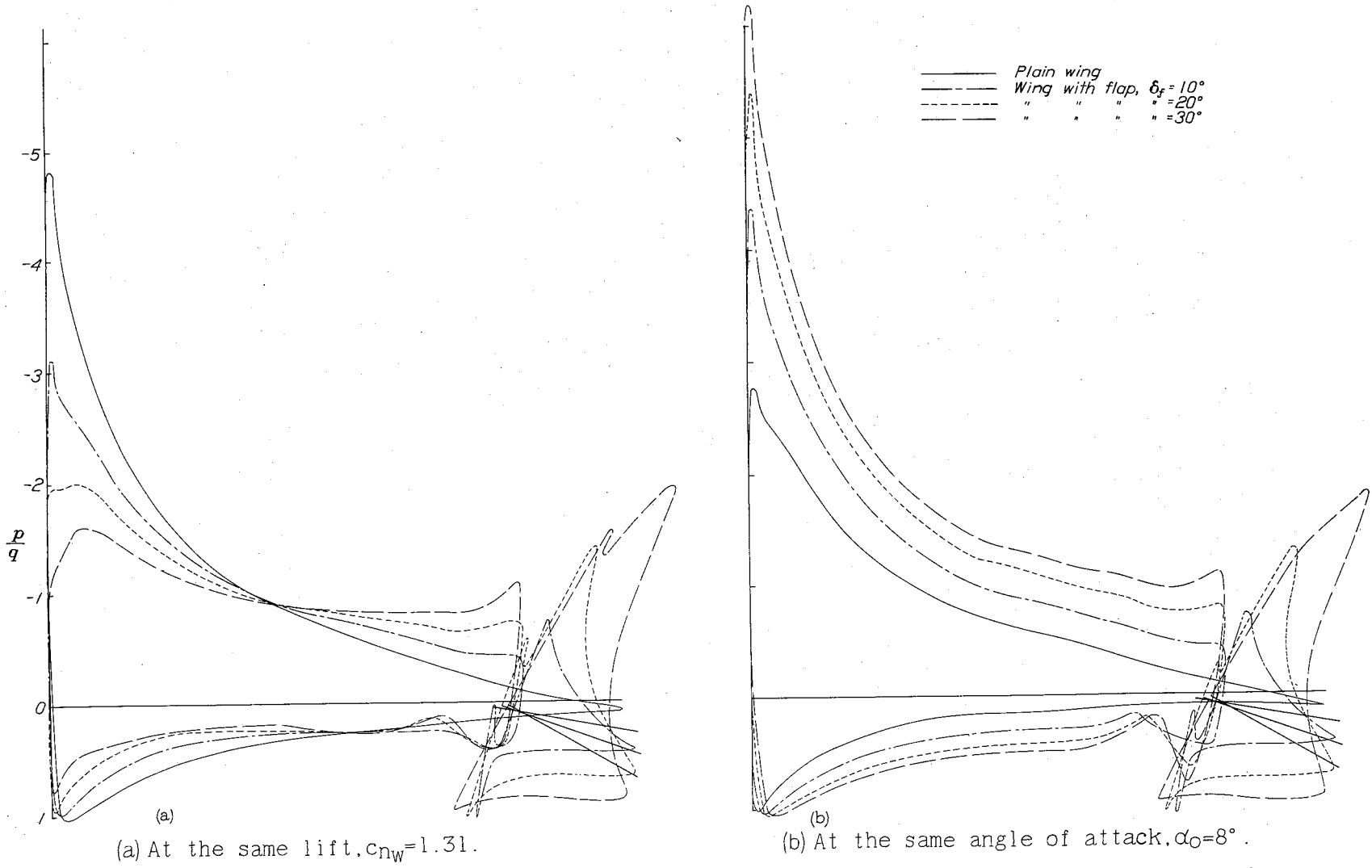


Figure 26.- Comparison of the pressure distribution on an N.A.C.A. 23012 wing and a 0.2566Cw slotted flap with that on the plain wing.

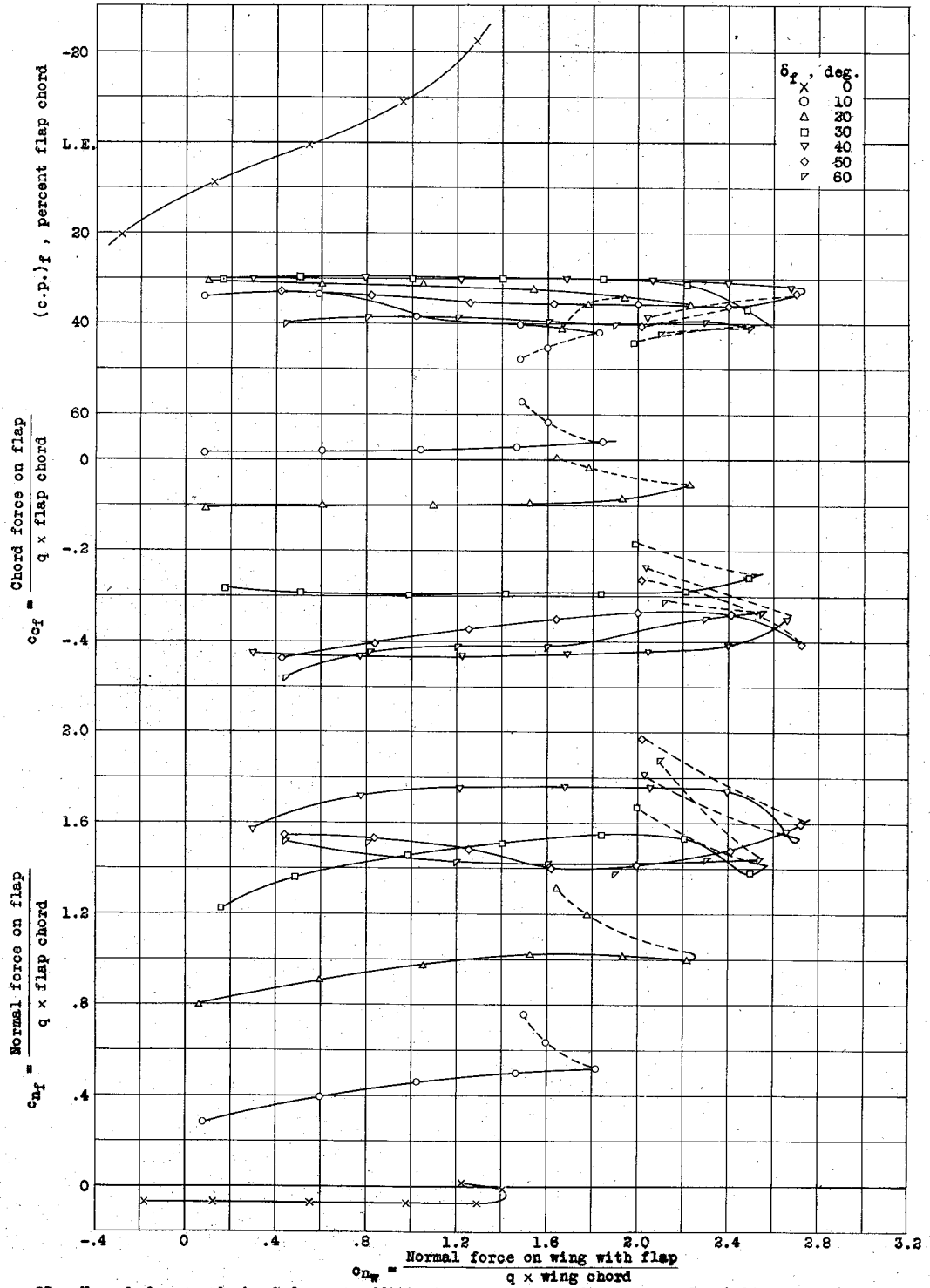
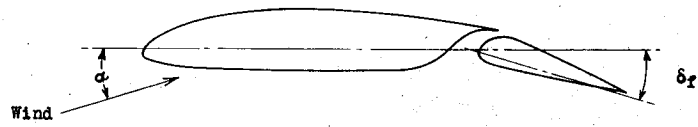


Figure 27.- Normal-force and chord-force coefficients and centers of pressure of a 0.2566  $c_w$  slotted flap on a N.A.C.A. 23012 wing, (reference 7).

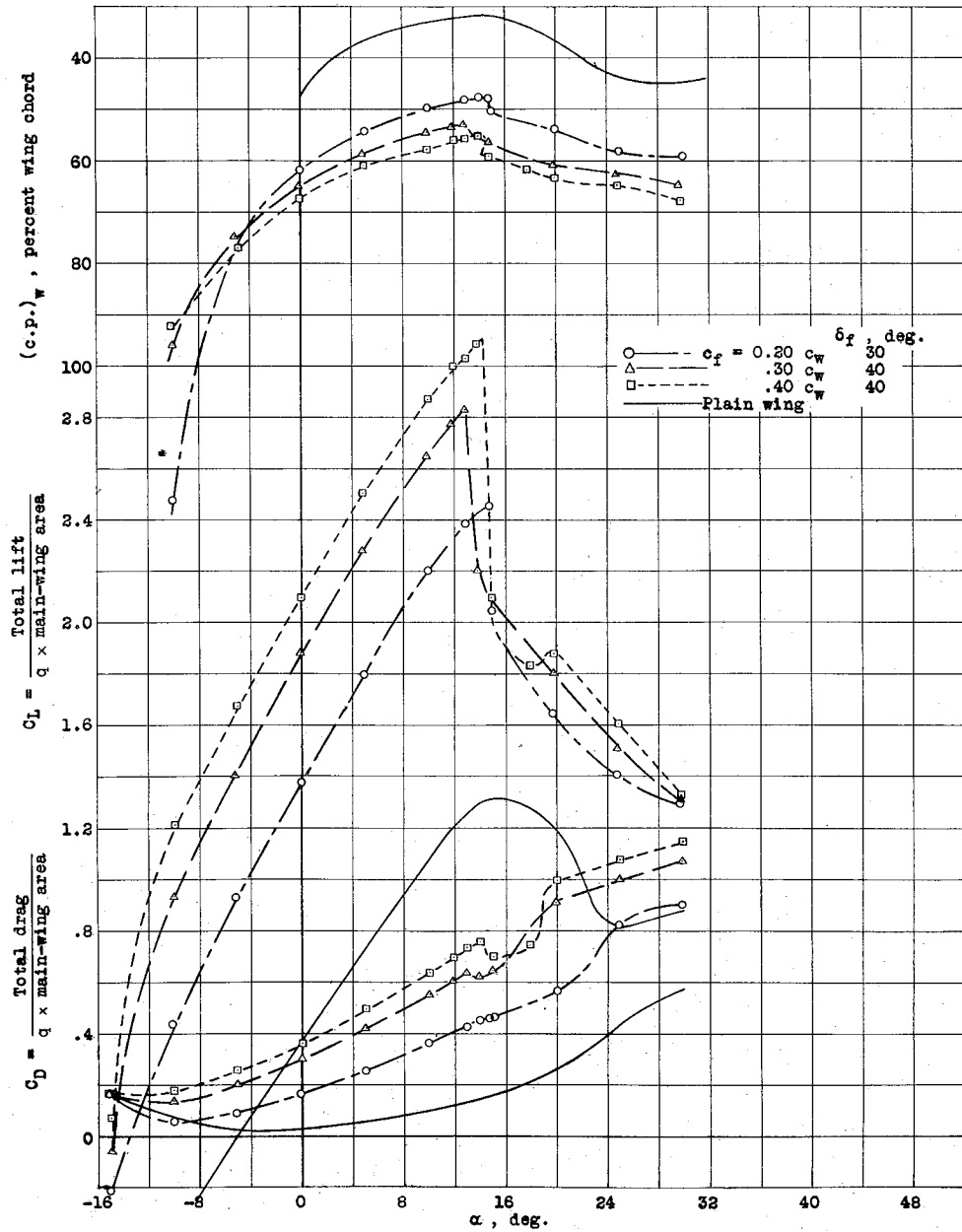
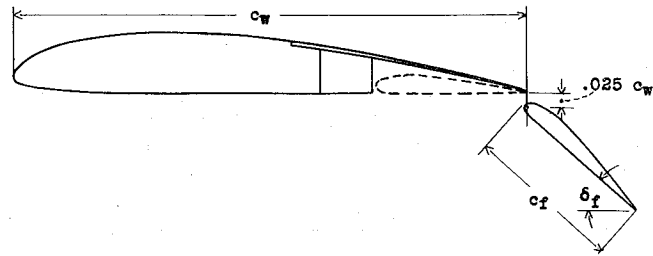


Figure 28.- Lift and drag coefficients and centers of pressure of a plain Clark Y wing and of a Clark Y wing with three sizes of Fowler flap, (reference 12).

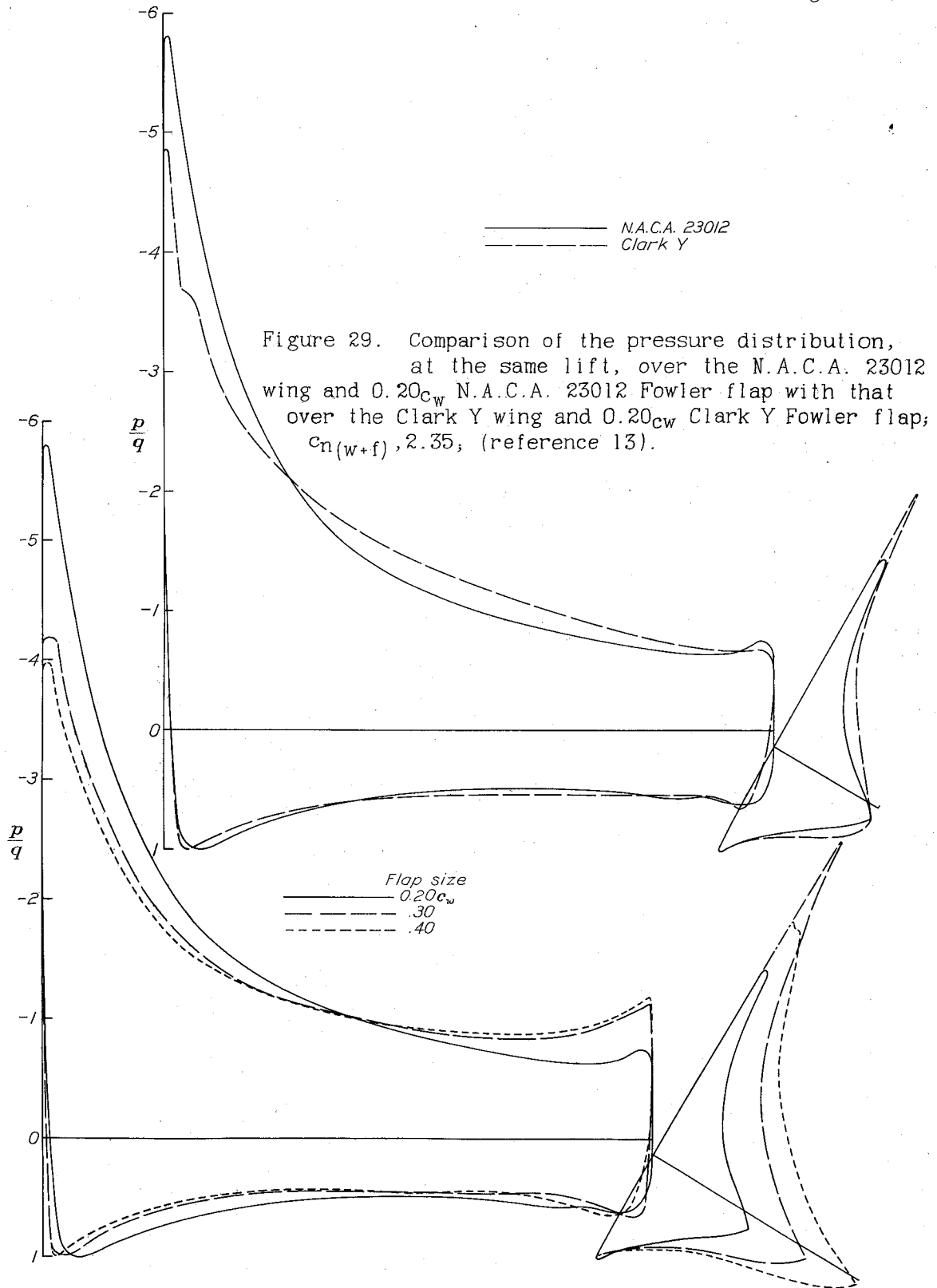


Figure 30. - Comparison of the pressure distribution, at the same lift, over the N.A.C.A. 23012 wing with  $0.20c_w$ ,  $0.30c_w$  &  $0.40c_w$  N.A.C.A. 23012 Fowler flaps,  $c_{n(w+f)}, 2.35$ ; (reference 13).

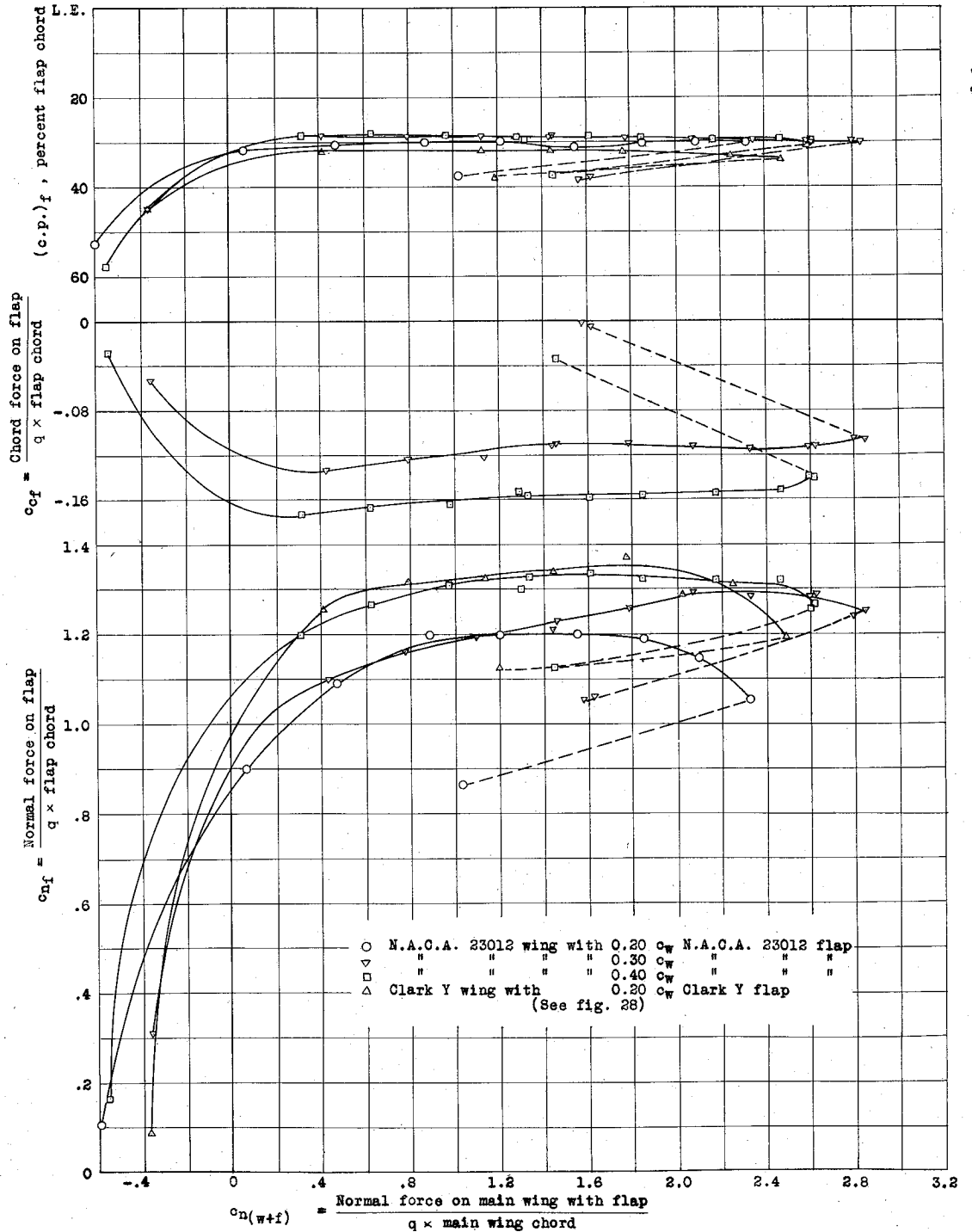
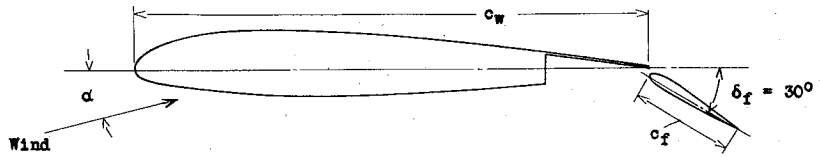


Figure 31.- Normal-force and chord-force coefficients and centers of pressure of Fowler flap on Clark Y and N.A.C.A. 23012 wings, (reference 13).

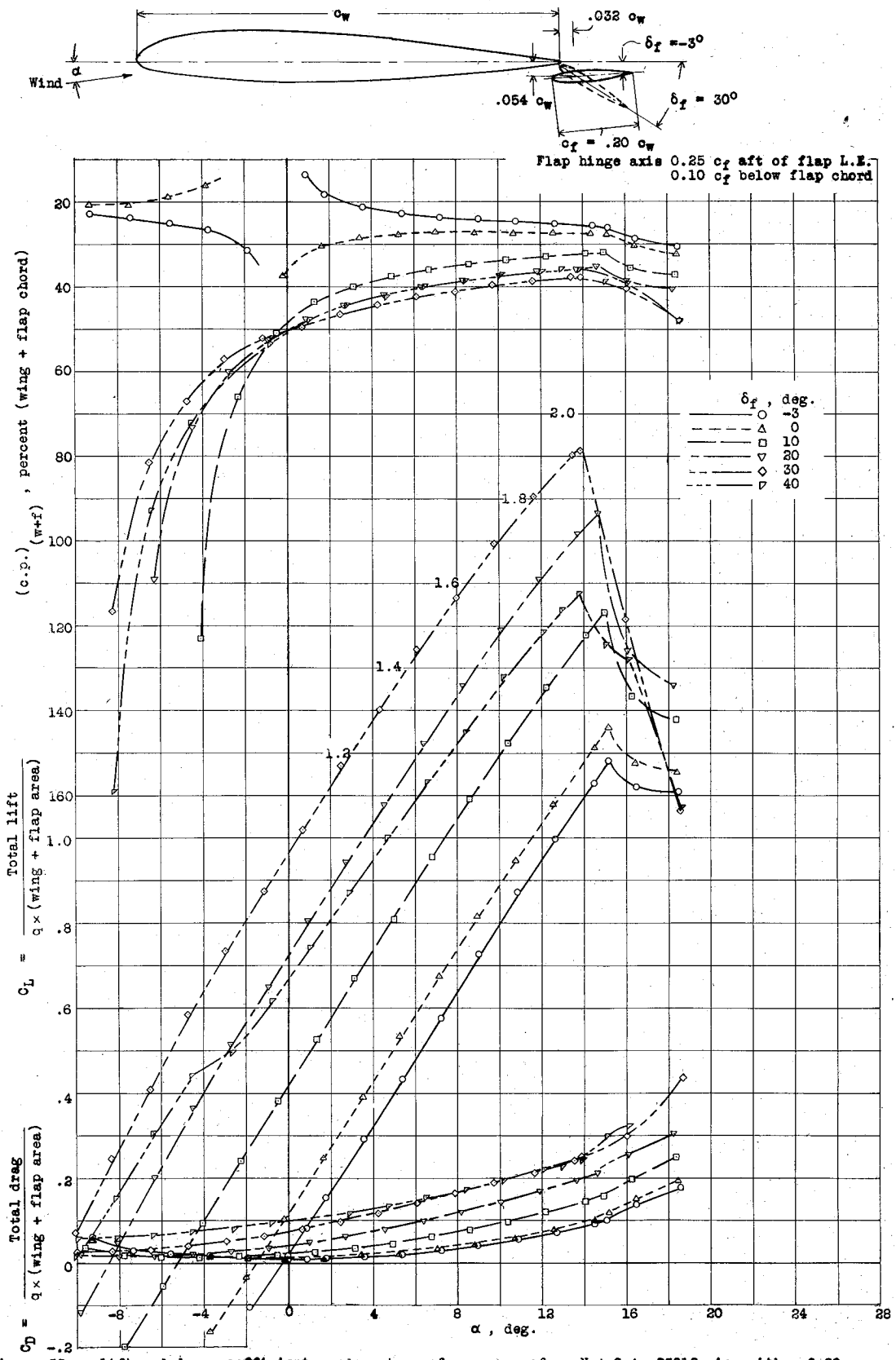


Figure 32. - Lift and drag coefficients and centers of pressure of an N.A.C.A. 23012 wing with a 0.20  $c_w$  N.A.C.A. 23012 external-airfoil flap, (reference 14).

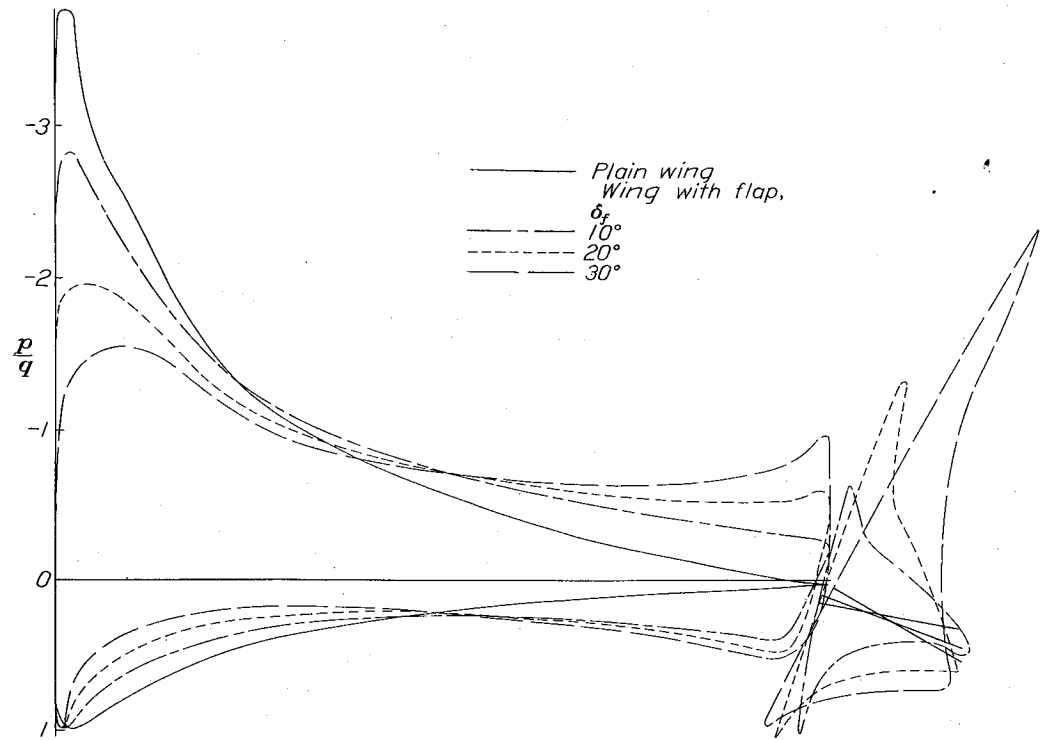


Figure 33. - Comparison of the pressure distribution over an N.A.C.A. 23012 wing with a  $0.20c_w$  external-airfoil flap with that over the plain wing at the same lift,  $c_n, l.165$ , (reference 15)

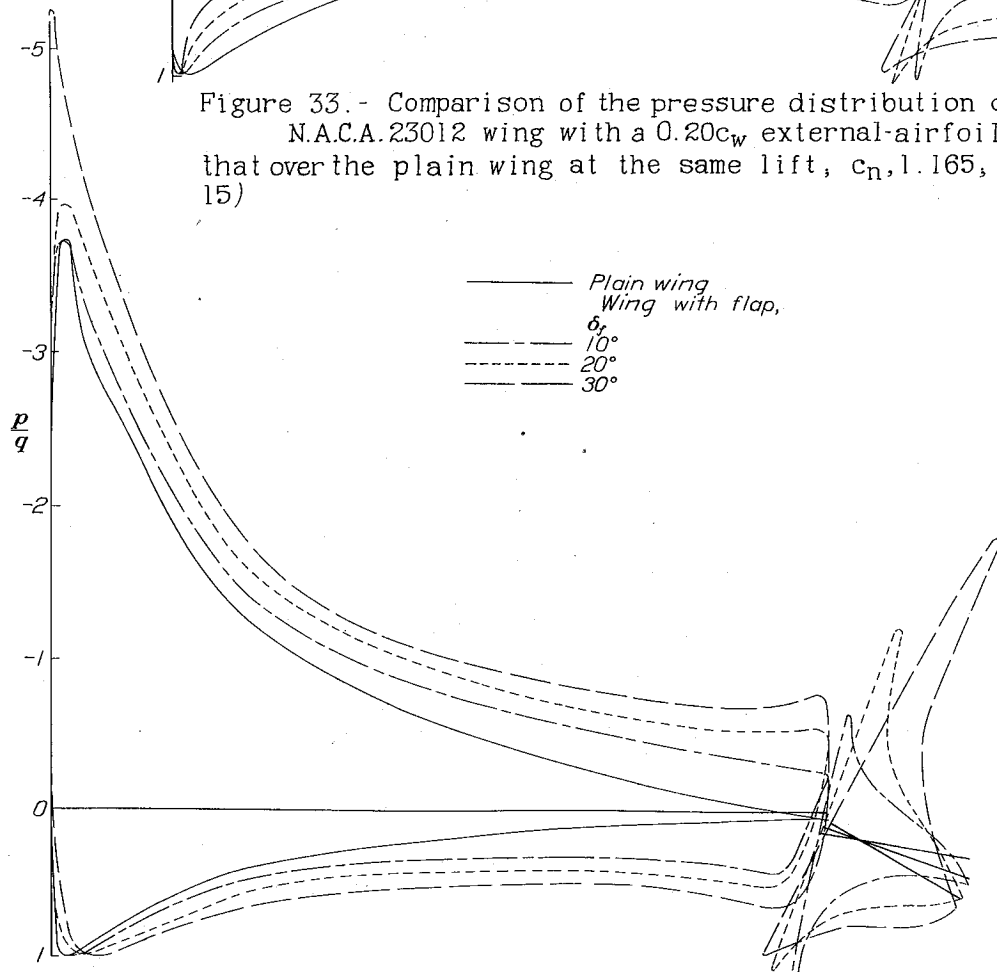
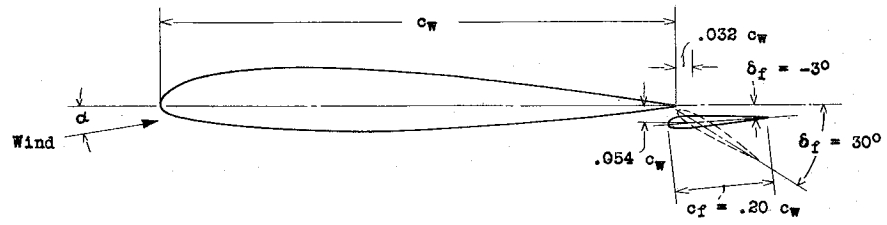


Figure 34. - Comparison of the pressure distribution over an N.A.C.A. 23012 wing with a  $0.20c_w$  external-airfoil flap with that over the plain wing at the same angle of attack,  $\alpha_0, 8.5^\circ$ , (reference 15).



Flap hinge axis 0.25  $c_f$  aft of flap L.E.  
0.10  $c_f$  below flap chord

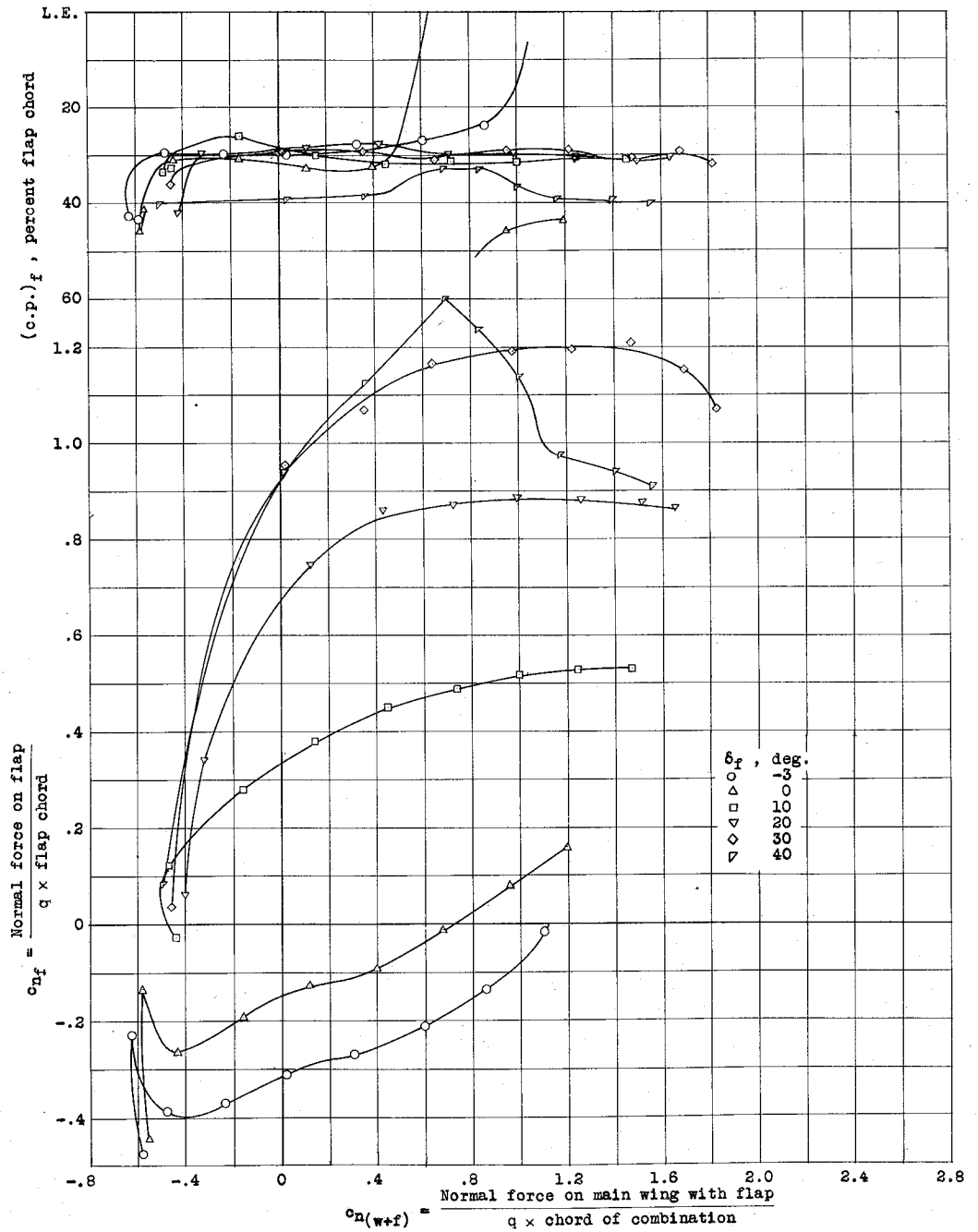


Figure 35.- Normal-force coefficients and centers of pressure of a 0.20  $c_w$  N.A.C.A. 23012 external-airfoil flap on a N.A.C.A. 23012 wing, (reference 15).